Energy Advances

ROYAL SOCIETY OF CHEMISTRY

PAPER

View Article Online
View Journal | View Issue

Cite this: *Energy Adv.*, 2022, 1, 402

SNG based energy storage systems with subsurface CO_2 storage

Stefan Fogel, *[a] Christopher Yeates,[b] Sebastian Unger,[a] Gonzalo Rodriguez-Garcia,[a] Lars Baetcke,[c] Martin Dornheim,[c] Cornelia Schmidt-Hattenberger,[b] David Bruhn[bd] and Uwe Hampel[ae]

Large-scale energy storage plants based on power-to-gas-to-power (PtG–GtP) technologies incorporating high temperature electrolysis, catalytic methanation for the provision of synthetic natural gas (SNG) and novel, highly efficient SNG-fired Allam reconversion cycles allow for a confined and circular use of CO_2/CH_4 and thus an emission-free storage of intermittent renewable energy. This study features a thorough technology assessment for large-scale PtG–GtP storage plants based on highly efficient sCO_2 power cycles combined with subsurface CO_2 storage. The Allam cycle employs supercritical CO_2 as working fluid as well as an oxy-combustion process to reach high efficiencies of up to 66%. The entire PtG–GtP process chain assessed in this study is expected to reach maximum roundtrip efficiencies of 54.2% (with dedicated and sufficient O_2 storage) or 49.0% (with a dedicated air separation unit). The implementation of said energy storage systems into existing national energy grids will pose a major challenge, since they will require far-reaching infrastructural changes to the respective systems, such as extensive installations of renewable generation and electrolysis capacities as well as sufficient subsurface storage capacities for both CO_2 and CH_4. Therefore, this study incorporates an assessment of the present subsurface storage potential for CO_2 and CH_4 in Germany. Furthermore, a basic forecast study for the German energy system with an assumed mass deployment of the proposed SNG-based PtG–GtP energy storage system for the year 2050 is conducted. In case of a fully circular use of CO_2/CH_4, when electricity is solely generated by renewable energy sources, 736 GW of renewables, 234 GW of electrolysis and 62 GW of gas-to-power capacities are required in the best case scenario in 2050. The total storage volume on the national scale of Germany for both CO_2 and CH_4 was determined to be 7.8 billion N m^3, respectively, leading to a CH_4 storage capacity of 54.5 TW h. The presented investigations illustrate the feasibility of large-scale energy storage systems for renewable electricity based on high temperature electrolysis, catalytic methanation and Allam power cycles paired with large subsurface storages for CO_2 and CH_4.

Received 25th October 2021,
Accepted 22nd May 2022

DOI: 10.1039/d1ya00035g

rsc.li/energy-advances

1. Introduction

The Intergovernmental Panel on Climate Change (IPCC) has estimated that anthropogenic global warming is already 1.0 °C above pre-industrial levels, and it is likely to reach 1.5 °C between 2030 and 2050.[1] Carbon dioxide (CO_2) is widely regarded as the greenhouse gas with the largest impact on global warming due to its large annual emissions of 33 gigatons (in 2019) worldwide.[2] Measures to cope with the exceeding CO_2 emissions include: (i) efficiency improvements in electricity use and generation; (ii) mass deployment of renewable electricity production as a low-carbon energy source or the continuing use of low-emission technologies such as nuclear power; (iii) capture of CO_2 from industrial processes including conventional energy production.[3,4]

Technologies such as carbon capture and storage (CCS) as well as carbon capture, utilisation and storage (CCUS) are viewed as key contributors in reducing anthropogenic CO_2 emissions and mitigating climate change by means of energetic reuse of CO_2 and sequestration in subsurface storages.[5–8] Sequestration is known as the process of injecting and storing CO_2 in geological subsurface storages over a geological time frame such as in depleted oil and gas reservoirs, coal beds, salt

[a] *Helmholtz-Zentrum Dresden-Rossendorf e.V., Bautzner Landstraße 400, 01328 Dresden, Germany. E-mail: s.fogel@hzdr.de, s.unger@hzdr.de, g.rodriguez@hzdr.de; Tel: +49 (0) 351 260 2254*
[b] *Deutsches GeoForschungsZentrum GFZ, Telegrafenberg, 14473 Potsdam, Germany. E-mail: yeates@gfz-potsdam.de, cornelia.schmidt-hattenberger@gfz-potsdam.de*
[c] *Helmholtz-Zentrum Hereon, Max-Planck-Straße 1, 21502 Geesthacht, Germany. E-mail: lars.baetcke@hereon.de, martin.dornheim@hereon.de*
[d] *Delft University of Technology, Stevinweg 1, 2628 CN Delft, The Netherlands. E-mail: david.bruhn@gfz-potsdam.de*
[e] *Technische Universität Dresden, 01062 Dresden, Germany. E-mail: u.hampel@hzdr.de*

caverns and saline aquifers.[9–13] It is a viable option to cope with CO_2 from large industrial emitters (*e.g.* conventional power plants, steelworks, cement plants and other large emitters) as well as CO_2 mitigation technologies, such as bioenergy coupled with CCS (BECCS), direct air capture (DAC) and others.[14–21] Carbon dioxide capture, temporary storage in subsurface reservoirs and its retrieval for reuse in fuel production is of relevance and represents an application of CCS technologies. Since CO_2 is inert, its subsurface storage is beneficial compared to the more reactive H_2 and monitoring experiments showed that the storage process is safe.[12,22]

The production of synthetic CH_4 *via* the Sabatier process (power to gas; PtG) through adiabatic fixed-bed methanation of CO_2 already reaches a TRL (technology readiness level) of 9.[23] The common step to any PtG or PtL (power to liquid) pathway is water electrolysis to provide the required H_2 for subsequent fuel syntheses. It represents the most important step from a technological perspective.[24–26] The most efficient technology can be found in high temperature electrolysis, utilising solid oxide electrolysis cells (SOEC). PtG is well suited for large scale-applications, demonstrated by several industrial scale pilot plants.[27–29] Hence, energy storage by means of CH_4 offers three major advantages: (i) it represents state of the art technology and can be deployed in the short term, (ii) novel and established power plant technology can be employed for the retransformation of CH_4 into electricity (gas to power; GtP), and (iii) the existing gas grid can be used for its storage and distribution, making it an energy carrier of outstanding significance for the energy transition process as well as the transformation of the industrial and transportation sector.[23,30]

The coupling of large-scale underground storage of CO_2 and CH_4 with the Sabatier process and conventional methane-fired gas turbine power plant technology for seasonal energy storage of renewables in Germany under the premise of a circular and emission-free use of both gases was previously introduced by works of Kühn *et al.*[30–32] Kühn *et al.* investigated the use of enhanced gas recovery (EGR) and the feasibility of mutual storage of CO_2 and CH_4 in the same subsurface reservoir demonstrating the viability of EGR and the interlaced energy storage concept. The predicted energy storage costs have been determined to be approx. 0.2 € kW^{-1} h^{-1} and it was found that the economic feasibility of the energy storage concept is not dependent on the subsurface storage operation itself but rather on the power-to-gas conversion step.[31,32] Specifically for the case of seasonal storage over a long time scale, the use of power-to-gas-to-power (PtG–GtP) shows competitive levelised energy storage costs in comparison to pumped storage hydroelectricity as shown in ref. 33 The roundtrip efficiency of the entire PtG–GtP process chain was expected to reach 28%, including a 4.7% efficiency drop caused by the energy expenses of the subsurface storage operation of CO_2.[30] Further studies by Kühn *et al.*[34] and Streibel *et al.*[35] concluded that the subsurface storage operation is insignificant with respect to the process chain efficiencies leading to losses of only 0.2% with roundtrip efficiencies of 26%. Other works further modified the previously mentioned concept on the process level, introducing a steam-based power generation cycle paired with oxy-combustion, enabling process efficiencies of 42% or even 54% when heat is decoupled from the system and used elsewhere.[36]

Power cycles based on alternative working fluids, such as supercritical CO_2 (sCO_2), are an attractive alternative to conventional steam-based thermal power generation cycles. As the pressure and temperature of the working fluid CO_2 at the turbine outlet is above the critical point (73.75 bar and 30.98 °C), the fluid density is high while the its viscosity is low. Thus, a more compact turbomachinery and equipment size can be achieved. Several studies have found a higher cycle efficiency compared to conventional steam Rankine cycles,[37,38] which results in a higher power-to-power efficiency and reduction in water usage. The semi-closed direct heated oxy-fuel power cycle, or so-called Allam cycle, offers an advantageous process layout. An oxy-combustion directly heats the sCO_2 stream to high temperatures and the process gases are then passed through the turbomachinery as well as the heat exchangers. Any water in the process gas stream is removed through condensation and as a result, the exhaust gas stream consists of pure CO_2. Hence, no additional equipment is required for the separation of CO_2 and high gas-to-power efficiencies can be achieved. The combination of the PtG process, the methane-fired Allam cycle and suitable large subsurface stores for CO_2 and CH_4 poses an enhancement over the system proposed by Kühn *et al.* regarding its roundtrip efficiency.[30,34]

As the end use of energy electrifies and the demand of electricity inevitably increases, energy systems predominantly based on renewable production will require flexible and large-scale energy storage systems, capable of compensating the mostly fluctuating electricity production from these sources. Aside from the capture and storage of large quantities of CO_2 and CH_4 as well as all previously laid out conversion steps for a closed-loop energy storage system, the constitution of the respective national and international electricity production infrastructures will play a crucial role in the efforts of achieving net-zero emissions by the mid of the century. Using the example of Germany, national studies predicting high shares of renewables ranging from 85 to 100% such as[39] and[40] in the upcoming decades, showed, that large-scale implementations of PtG–GtP plants can help to reduce grid congestion and to store electricity over longer periods of time. According to Thema *et al.*, a PtG capacity of 89 to 134 GW and a renewable capacity of up 290 GW is required until 2050 in a 100% renewable scenario for the German electricity sector.[40]

This work presents the first description of the combination of PtG–GtP energy storage processes and Allam power cycles with subsurface storages and a confined usage of CO_2/CH_4, extending previously discussed works. The performance of the proposed energy storage system is determined *via* a thorough technology assessment. Based on a simplified system model, an energy system forecast study is conducted and key system requirements are determined and the implications of the mass deployment of the PtG–GtP system in conjunction with large subsurface stores are discussed for the first time.

2. Study objectives

This paper assesses a concept of a highly efficient energy storage system based on high temperature electrolysis for the production of H_2 and the catalytic methanation of CO_2 for the production of synthetic CH_4, paired with an advanced SNG-based power generation cycle employing supercritical CO_2 (sCO_2) as a working fluid. During the operation of the system, the required carbon inventory will be kept in a closed material cycle utilizing large-scale subsurface stores for the storage of CH_4 and CO_2. Assuming the sole use of renewables for the storage cycle of the system and no external carbon sources, the proposed system allows for a fully emission-free storage and production of electricity. In the following sections, relevant technological choices with respect to power storage (power to gas), power generation (gas to power) and storage of CO_2, CH_4 and other relevant gases are presented and discussed. Furthermore, the potential for geological storage of CO_2 in Germany is analysed.

Based on the presented technology choices, an exemplary forecast study of the development of the German energy system is conducted based on historical weather and electricity production data. A projection of the energy system until the year of 2050 is carried out assuming that the overall national electricity storage and production requirements are covered by the aforementioned energy storage system. The forecast is used as an orientation study to determine the required renewable, PtG and GtP capacities as well as the required subsurface storage capacities for CO_2 and CH_4 on a national scale and to evaluate the plausibility of the overall concept for a large-scale deployment.

3. Plant concept

3.1 Overview

The energy storage plant consists of two sections: power to gas (PtG), and gas to power (GtP). As their operation is asynchronous, large-scale storage of both CH_4 and CO_2 is required (Fig. 1). Due to the confined technical use of CO_2 and CH_4 in a closed loop, the energy storage plant is characterised by no directly associated atmospheric emissions of both gases.

During periods of negative residual load, while renewable production exceeds the current load requirements of the energy system, the produced electricity is used in the PtG section, consisting of a water electrolyser coupled with a methaniser to produce H_2 and subsequently CH_4 according to eqn (1) and (2).

$$H_2O \rightarrow \frac{1}{2}O_2 + H_2 \quad (1)$$

$$CO_2 + 4H_2 \rightarrow CH_4 + 2H_2O \quad (2)$$

The required CO_2 for the Sabatier reaction eqn (2) is drawn from a large subsurface storage facility, *i.e.* porous aquifers or caverns. The overall reaction of this process step is formulated in eqn (3).

$$2H_2O + CO_2 \rightarrow CH_4 + 2O_2 \quad (3)$$

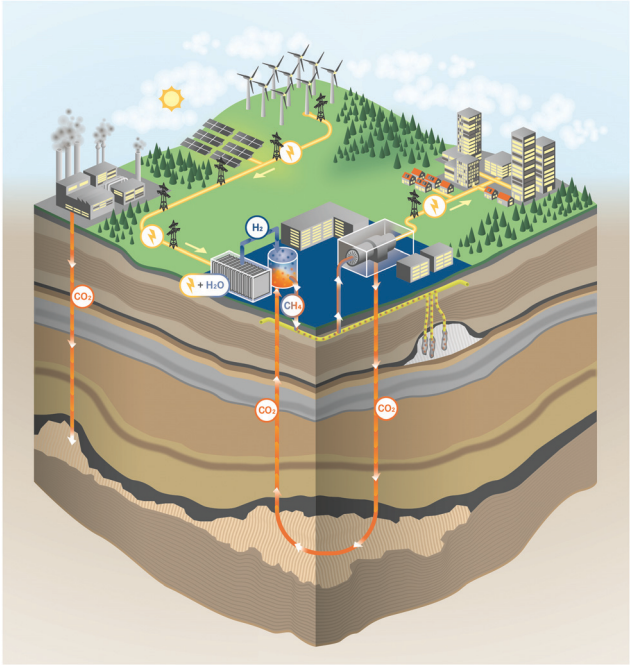

Fig. 1 Carbon loop of the energy plant based on subsurface gas storage.

The produced CH_4 is temporarily stored in a suitable subsurface storage facility that is comprised of caverns. The technical characteristics and details of the PtG cycle can be found in Section 3.2.

During times of positive residual load, while the load requirements of the energy system exceed the current renewable electricity production, CH_4 is extracted and burnt in the GtP section according to eqn (4).

$$CH_4 + 4O_2 \rightarrow CO_2 + 2H_2O \quad (4)$$

This section consists of an oxy-combustion power cycle, where supercritical CO_2 is used as a working fluid and oxygen is either provided from a dedicated O_2 storage or generated by an air separation unit (see Section 4.2). Details regarding suitable power cycles will be discussed in Section 3.3. Thus, the carbon loop of the energy plant can be seen as the counterpart of its electric cycle: CO_2 is extracted from the storage when renewable electricity is available in the electricity grid. During times of exceeding electricity demand, the subsurface CO_2 storage is charged.

Considering this circular approach to a carbon inventory of fixed size and to a fully decarbonized national energy system, it is apparent that, besides the large capacities for renewable energy production and electrolysers, large storage capacities for CO_2, CH_4 and O_2 as well as for the intermediate appearance of H_2 is necessary. Furthermore, H_2 storage becomes necessary for other applications (*e.g.* steel production, chemical industry, refuelling infrastructure). Possible solutions for gas storage are discussed in Section 3.4. The flow chart for the investigated system structure based on an SOEC and a power cycle employing sCO_2 as a working fluid is shown in Fig. 2.

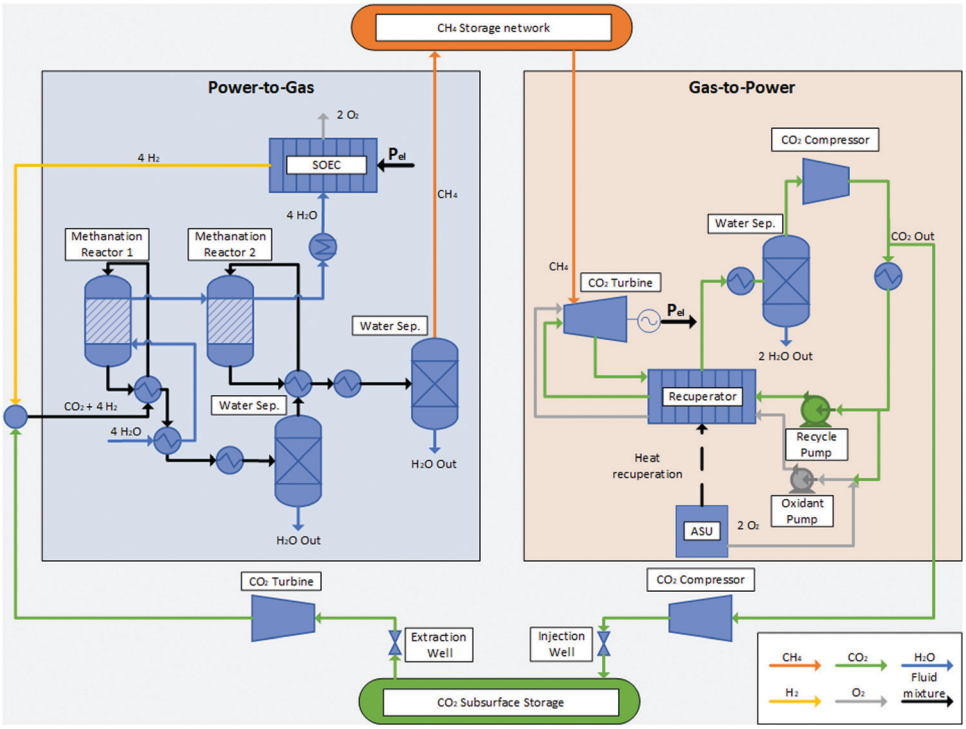

Fig. 2 Flow chart of the combined PtG–GtP and subsurface storage energy plant.

3.2 Power to gas cycle

Since the production of H_2 from renewables within a fully decarbonised national energy system is widely regarded as the main contributor of the consumption of electricity, the choice of the respective electrolyser technology has a major impact on the overall efficiency of a PtG–GtP-system.[41] A brief comparison of different electrolyser technologies is carried out in Table 1.

Solid oxide electrolyser cells (SOEC) gained major attention in recent years.[50–52] Making use of a membrane electrode assembly (MEA) comprising dense ceramic electrolytes that can be either oxygen-anion or proton conducting as well as porous cermet electrodes, SOECs can produce wet or dry H_2 at temperatures between 500 °C and 1000 °C.[52–54] SOECs surpass todays commercialised electrolyser technologies such as AEL and PEM with respect to cell voltage, efficiency and specific power consumption (Table 1). However, the main advantage of SOECs lies in the thermal integration of downstream waste heat streams into the process, which is of particular interest and benefit in conjunction with process combination presented in this work. The employed Allam cycle offers waste heat at high temperature levels, which can be used within the SOEC stage. This leads to higher system efficiencies, especially when combined with downstream chemical syntheses such as methanation or methanol synthesis.[55–59] The obtainable efficiency of SOECs incorporating thermal integration depends on a wide variety of factors, such as the composition or characteristics of the employed ceramic as well as the operating parameters of the SOEC stack. Considering heat recovery, electrolyser standalone efficiencies up to 90% and even close to 100% can be achieved.[41,60]

The most common technology for the synthesis of CH_4 is the thermocatalytic conversion of H_2 and CO_2 *via* the Sabatier reaction eqn (2). The thermocatalytic methanation by means of an evaporation-cooled polytropic fixed-bed reactor has reached the stage of industrial applications (TRL 9) so far and is currently assessed in large scale demonstration plants.[23,42,61]

Table 1 Comparison of electrolyser technologies[29,42–49]

	AEL	PEM	SOEC
Development state	Commercialised	Demonstration/commercialised	R&D
Electrolyte	NaOH, KOH	Polymer	Ceramic
Charge carrier	OH^-	H_3O^+/H^+	O^{2-}/H^+
Cell temperature in °C	40–90	20–100	600–1000
Cell voltage in V	1.8–2.4	1.8–2.2	0.91–1.3
Efficiency HHV in %	50–60	55–82	40–86
Current system power consumption in kW h N^{-1} m^{-3} H_2	4.5–7	4.5–7.5	2.5–3.5
Part load capability/transient operation	Part load operation possible; not well suited for transient operation	Partial load and overload operation possible; well suited for transient operation	Transient operation not viable

Several research activities focus on a direct and thermally integrated coupling of SOECs and methanation reactors. Their focus lies on the reuse of the steam generated in the cooling system of the Sabatier reactor as feed stream in the SOEC stage. The rather low temperature of steam (approx. 250 °C) offers no suitable heat source for gas pre-heating through the implementation of additional heat exchangers, but can be used to replace dedicated water evaporators for the SOEC feed. Based on demonstration scale experiments, Gruber *et al.* showed overall PtG efficiencies up to 82% using this kind of thermal integration.[59] Theoretically, efficiencies up to 86% can be achieved for the PtG process based on methanation.[60,62]

3.3 Gas to power cycle

The conventional power generation cycle compensates positive residual loads in case of insufficient renewable electricity production. Three possible routes are considered for the power generation in the present study as shown in Fig. 3. The state-of-the-art technology (Fig. 3a) is a conventional gas power cycle with post combustion carbon capture. Air and the synthetic CH_4 are combusted to drive an open gas turbine cycle. The exhaust gas stream transfers the heat to a bottoming cycle to utilize the remaining thermal energy. From the exhaust gas stream CO_2 is separated, which can be done for example *via* scrubbing. In case of the two other routes, CH_4 and O_2 will be used in an oxy-combustion process to drive the power cycle directly or indirectly. The O_2 can be generated by an air separation unit (ASU) or from an O_2 storage, which was initially filled by the electrolysis (Fig. 3b and c). The exhaust gas stream consists of H_2O and CO_2. A separation of CO_2 requires less energy compared to the conventional process, since the H_2O can be removed by condensation.

Gas-fired power generation contributes to 23% of the overall power generation worldwide, mostly using CH_4 as fuel.[63] Gas turbines have become the preferred power generation technology due to their high cycle efficiency, small installation time, and low level of CO_2 emissions compared to other conventional alternatives.[64] There are several technical concepts of gas turbine power cycles, such as the simple gas turbine process, the steam injected gas turbine process, the humid air turbine process as well as the combined gas and steam turbine process. Due to the high process efficiency, the latter is the state-of-the art nowadays. Thus, it is analysed in more detail below.

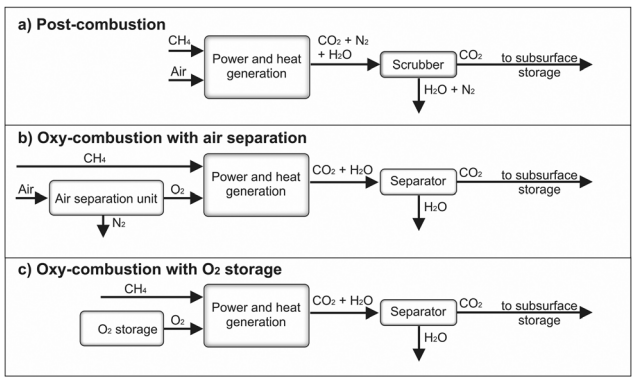

Fig. 3 Process routes for heat and power generation including CO_2 separation.

The synthetic CH_4 is injected with pressurized air into a combustion chamber. The combusted gas mixture drives a turbine with an inlet temperature up to 1500 °C and reduces down to 500 °C during expansion.[65] The exhaust gas stream from the gas turbine outlet transfers the thermal energy to a water/steam based power cycle, also known as bottoming cycle, and is released to the environment. The evaporated water drives a steam turbine, condenses at the turbine outlet and is recirculated to the exhaust-water heat exchanger. The optimization of these cycle configurations is subject of several investigations.[66–68]

An upcoming alternative for the bottoming cycle is a thermal power cycle using sCO_2 as a working fluid. Numerous studies have shown that sCO_2 based power cycles have the potential to achieve higher cycle efficiency compared to conventional steam Rankine cycles.[37,38] A higher power generation efficiency will eventually result in higher power-to-power efficiency and lower cooling water usage. Furthermore, the high density of the working fluid leads to small equipment size and footprint of the power generation unit. There are several possible sCO_2 power cycle layouts, such as recuperation, intercooling, reheating and recompression. A more detailed investigation of the existing layouts can be found in ref. 69–71.

The sCO_2 power cycles benefit from the fluid properties of CO_2. For instance, a lower pressure and temperature near the critical point strongly reduces the required compression work and enhances the cycle efficiency. A comparison in between these two cycles based on system analysis shows a higher efficiency of the sCO_2 cycle, when the turbine inlet temperature exceeds approximately 425 °C, which is the case for a gas turbine exhaust stream or the exhaust stream of a combustion chamber.[72] Summarizing, sCO_2 power cycles are promising technologies to convert chemical energy into electrical energy.[71,73]

The described cycles achieve a high thermal efficiency within the existing power plant technologies.[64] Nevertheless, additional expensive, efficiency-reducing equipment is required in order to capture CO_2 and other pollutants from the exhaust gas stream. This separation equipment reduces the overall efficiency and increases the cost of electricity by 50% to 70%.[74] As a result the power cycle efficiency will be between 47.7% and 48.8%.[75]

The semi-closed direct heated, oxy-fuel Brayton cycle offers some advantages over the indirect heated closed Brayton cycle. In the former, the working fluid consists only of CO_2 and H_2O, due to the oxy-combustion. Due to a pressure below the critical point, CO_2 is not in its supercritical phase. The separation of CO_2 and H_2O after expansion requires less energy and avoids the emission of NO_x. CO_2 or H_2O are recirculated and used as moderator gas in the combustion chamber, leading to a reduction of the turbine inlet temperature. The efficiency of these oxy-combustion power cycles and the CO_2 separation is between 48.9% when an air separation unit is taken into account and 53.6% without air separation unit.[76,77]

A power cycle using sCO_2 as a moderator gas is also known as Allam Cycle. In such a cycle, the recycled CO_2, CH_4 and O_2 enter a combustion chamber and the temperature increases up to 1150 °C at 300 bar pressure during combustion. The sCO_2 and H_2O gas mixture expands to 30 bar and 700 °C in the turbine. The exhaust flow enters a recuperating heat exchanger to preheat the high-pressure CO_2 recycle stream. From this recuperator, the exhaust gas is cooled to near ambient temperature and water is separated. The remaining CO_2 stream is recompressed to 300 bar and approximately 5% of the pure CO_2 is exported to the subsurface storage. The remaining CO_2 flow is cooled, partially mixed with O_2, and pumped through the recuperator to reheat by the hot turbine exhaust gas flow. This preheated gas mixture enters the combustion chamber and the process repeats.[78] The energy required for the ASU to generate the O_2 was taken into account and the power cycle achieves an efficiency up to 59.8% at low capital cost.[79] However, if it is possible to supply the power cycle with stored O_2 provided by the electrolysis section, an increase of the net cycle efficiency to 66.1% can be achieved.[80]

Table 2 shows a comparison of the previously described power cycle technology choices and the achievable roundtrip efficiencies for the PtG–GtP system based on a PtG efficiency of 82% as shown in ref. 59. The PtG–GtP system paired to an Allam cycle with dedicated O_2 storage is characterised by a maximum roundtrip efficiency of 54.2% whereas the same configuration with a separate ASU reaches roundtrip efficiencies of up to 49.0%.

The PtG–GtP efficiency is also known as round-trip-efficiency and commonly applied for energy storage systems. Furthermore, the cost in terms of capital expenditures of storage technologies is a relevant parameter for their economic evaluation. In order to rank the presented long-term energy storage system, data from literature were analysed and listed in Table 3.

As one can see, the pumped hydro storage is a well-developed technology, which reaches high efficiency at low cost and can be considered as a reference case. However, the potential locations for installation of pumped hydro storages are limited and further storage technologies are required. In the study of Abdon *et al.*,[33] the long-term storage of H_2 would require large capacities, which cannot be provided by technical storages. Thus, an injection of H_2 into the gas grid (to limited extent) as well as a reformer to convert the gas mixture was considered. As a result, a power-to-CH_4 storage achieves higher efficiencies and lower cost compared to a power-to-H_2 storage system. On the other hand, Jülch[81] studied a cavern storage for both, H_2 storage and CH_4 storage. Here the CH_4 storage was considered to be approximately 3 times more expensive, without cause. Furthermore, additional cost for a CO_2 purification plant were considered for the power-to-CH_4 storage system, which is not needed in the presented energy storage concept. It becomes clear, that the presented energy storage system achieves higher efficiencies and does not require additional gas reformers or CO_2 purification. Furthermore, the geothermal energy input into the stored CO_2 may enhance the methanation process efficiency. Hence, potentially lower costs at higher efficiencies can be expected for the presented concept. Though efficiency and cost are crucial parameters for evaluating various storage technologies, other parameters such as energy density, reliability, lifetime and storage capacity are also relevant. Thus, for determining the optimum storage technology several aspects need to be considered, specifically thorough techno- and thermo-economic analyses. Therefore, a thermo-economical investigation will be conducted in subsequent studies.

Table 3 Comparison of the expected efficiencies and cost of long-term energy storage technologies

Storage technology	Pumped hydro storage		Power-to-H_2 storage		Power-to-CH_4 storage	
Ref.	81	33	81	33	81	33
Efficiency	76%	78%	41%	22%	32%	27%
Capital expenditures [EUR kW^{-1}]	800	1250	1372	3189	1802	1901

3.4 Gas storage options

Gas storages can be categorised in: (i) subsurface stores based on natural and artificial underground structures, such as porous aquifers or salt caverns and depleted oil and gas reservoirs, and (ii) technical gas storages, such as pressurized tanks or cryogenic storage of liquefied gases. The previously discussed PtG–GtP technology options require large storage capacities for CH_4 and CO_2. Hence, technical storages for CH_4 and CO_2 lie outside the scope of this study. Due to the expected asynchronous operation of the process steps of the PtG–GtP plant and further operational cases, such as start-up, shutdown and component failure, additional gas storages are vital to the overall plant design, with other relevant gases being O_2 and H_2.

Cavern and aquifer storages differ with respect to their geological and limiting availability as well as their development and operational cost. Typically, caverns offer faster rates of gas deliverability, and an increased number of injection–extraction

Table 2 Comparison of gas fired thermal power generation cycles and the achievable PtG–GtP efficiencies

Cycle	Combustion	Working fluid sCO_2	GtP efficiency (%)	Ref.	PtG–GtP efficiency (%)
Combined cycle	Post-combustion	No	50.0–50.7	66–68	41.0–41.6
Combined cycle	Post-combustion	Yes	50.0	71 and 73	41.0
Combined cycle	Oxy-combustion	No	48.0–49.3	68, 75 and 76	39.4–40.4
Allam cycle with ASU	Oxy-combustion	Yes	55.1–59.8	75, 76, 78–80	45.2–49.0
Allam cycle	Oxy-combustion	Yes	66.1	80	54.2

cycles per year. However, caverns require a larger initial capital investment for their development, typically multiple years of leeching, as well as water treatment for the produced water during the leeching process. The costs associated with temporary aquifer storage development involve large data acquisition and geological characterisation as they have not been previously explored for use. Aquifer stores require large amounts of cushion gas (up to 90% of overall volume), which could however be seen as an opportunity here to unload an initial amount of CO_2 outside of the synthetic fuel loop. Finally, a significant amount of water is also expected within porous aquifer development and operation, which will need to be cleaned and disposed of at cost. Depleted oil and gas fields, while only available at a handful of locations, offer reduced costs compared to porous aquifers due to their previous use which reduces the costs associated with characterisation and water production.[82]

Storage of CH_4. Options for temporary storage of high energy density gases such as CH_4 are numerous and technologically mature. In terms of underground gas storage (UGS), facilities have been historically built on depleted oil and gas fields or saline aquifers worldwide, injecting gas into porous rock networks in structurally advantageous geological locations for easy recovery. Such stores have made up most of the underground storage volume until recently. Currently, 16 porous storage formations are in use in Germany, comprising a total usable volume 8.6 billion N m^3.[83] Using salt caverns for gas storage, classically used for liquefied petroleum gas, offers a higher deliverability and a lower cushion gas requirement than porous stores. Despite larger initial investment costs relative to porous stores, caverns have been employed to a much higher degree in the last decades.[84] The largest cavern storage facilities in Germany, such as the Bernburg facility, operated by VNG Gasspeicher GmbH, and the Epe-Uniper facility, operated by Uniper Energy Storage GmbH, combine more than 30 individual caverns in an integrated storage system.[83]

Finally, surface storage of gas is also well established through either storage in tanks of liquefied natural gas (LNG) or overloading the pipeline network itself with increased gas pressure. The amount of gas that can be stored in surface stores is however notably lower than their underground counterparts.

Storage of CO_2. Permanent underground CO_2 storage is a method of disposing of CO_2 through direct injection of purified CO_2 into deep porous rock. CO_2 is initially trapped in the rock matrix in gaseous form, dissolves in the formation water (medium term), but ultimately mineralizes and solidifies as part of the rock itself (long-term). Due to their relative abundance, deep saline aquifers offer massive and easily accessible storage capacities.[9,85–87] Multiple successful offshore and onshore CO_2 storage pilots and full-scale operations have occurred or are ongoing worldwide.[88] The largest injection on the German territory is the Ketzin CO_2 pilot site in which more than 67 kilotons of CO_2 were injected over the course of 5 years.[89]

Recoverable CO_2 storage presents a different but nonetheless related set of geological requirements to permanent CO_2 storage in porous rock. While in both cases, the existence of a thick, high porosity storage layer sealed by a low permeability barrier layer directly overhead is vital, the necessity of a well-formed structural trap is less important in the permanent storage case, as the injected CO_2 is expected to form a considerable areal plume within the storage layer without any prospect of recovery. Finally, permanent CO_2 storage is mostly done in deep (>800 m) layers in which CO_2 reaches a supercritical state due to the favourable pressure–temperature environment at such depths, ensuring greater injectivity while reducing hypothetical interaction with shallower layers.

In Germany, a large potential for permanent CO_2 storage has been identified[90] and many potential stratigraphically successive storage-seal pairs have been located with sufficient thicknesses across the onshore and offshore territory.[91]

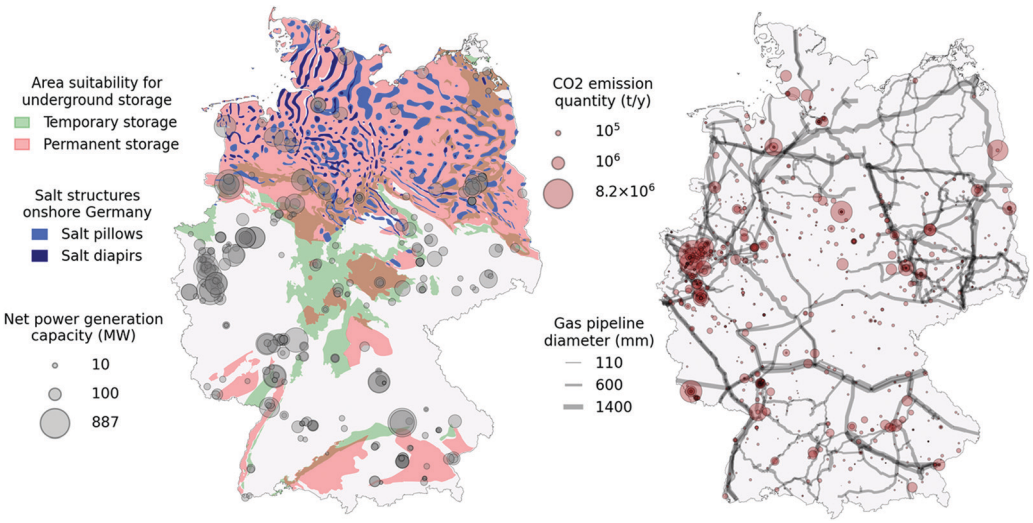

Fig. 4 Map showing relevant underground storage potential for salt structures and porous rocks. Point sources showing quantities of emitted CO_2 registered within the ETS are shown as grey circles.

The overall onshore and offshore storage potential in Germany has been estimated to lie between 20.4 and 115.3 gigatons of CO_2. A summarising map of the onshore CO_2 storage potential can be seen in Fig. 4 (left). The data originates from a study and data release by the German Federal Institute for Geosciences and Natural Resources.[90] This map was established by joining the various surface zones that bear storage-capable layers meeting a series of geological criteria. This map layer is labelled ''Permanent storage''. Zones that bear shallower storage-capable layers with less stringent criteria were similarly joined in a single map layer shown as ''Temporary storage''.

Temporary storage zones are shallower than permanent storage zones and have a depth of less than 800 m. This depth roughly marks the transition of stored CO_2 from a gas to a supercritical state. For that reason, CO_2 possesses lower density and buoyant forces reduces injectivity and CO_2 might remain closer to the injection location and can be more easily recovered. In both cases, the porosity of storage rocks must be above 10%, and average permeabilities above 10 mD, while often being higher. Storage rock thickness must be at least 10 m. The permanent storage layers must furthermore have a storage rock upper depth of at least 800 m and a barrier rock thickness of at least 20 m. Well-established low permeability rocks, such as salt and clay layers, were considered as barrier rocks. A pre-requisite for any use of the underground is in-depth local geological characterisation to establish safe operation. Further geological characterisation may reveal new knowledge regarding the underground storage potential and as such these maps are subject to change. While a large portion of the German onshore territory is covered by potential storage zones, areas devoid of deep storage capacity are observed, notably in North Rhine Westphalia, in which most existing power plants are found.[90]

The same map (Fig. 4, left) shows the identified salt structures that could potentially sustain salt caverns for temporary CO_2 storage.[92] Salt caverns are artificial cavities created by dissolving solid underground salt layers with freshwater. As such, the process is only feasible in specific salt formations. In Germany, the Zechstein formation, currently largely unused, provides ample possibilities for salt caverns, achieving sufficient thickness in large areas spread over most of the Northern half of Germany, with the inclusion of very thick salt diapirs in the Northwest region. There are currently 31 cavern storage facilities comprising a usable volume of 27.4 billion N m^3. According to some estimates, German cavern storage potential accounts for up to 42% of all European storage potential.[93] Salt caverns are currently used for temporary storage of high value gases such as CH_4 due to the high initial investment costs.

Finally, gas-fired power generation facility locations and corresponding net power generation capacity for the year 2020 are displayed.[94] Through this map, we can get an impression of good candidates for our system concept displaying high power generation capacity and storage potential at the same location. On another map (Fig. 4, right), CO_2 emitters originating from industry and registered within the European Trading Scheme (ETS) for the year 2018 are shown as translucid red circles.[95] Emitters whose primary function is energy production are not included in this map. Instead, harder-to-abate industry sources are shown as potential to supply the proposed plant concept with CO_2 specifically for the compensation of potential losses during the system operation. The 2020 gas pipeline network[96] (showing pipelines with diameters above 100 mm) is also given, indicating CO_2 pipeline network layout possibilities linking industry sources to plant or storage locations. Overlapping pipelines appear darker as individual pipelines are drawn with some transparency.

Furthermore, a basic energetic assessment was done in order to evaluate the input of the geothermal temperature and pressure within a deep porous storage. The temperature as well as the pressure inside the geological structure strongly depends on its depth. The sCO_2 leaves the power cycle at a pressure of 100 bar and a compression is not required for storages at shallower depths than 1000 m. In case of deeper storage of *e.g.* 5000 m the sCO_2 needs to be compressed and will be heated in the process. Therefore, a thermal storage will be beneficial before the CO_2 is stored in the underground. Since the temperature of the geological structure is at approximately 180 °C, the CO_2 will be heated during the storage. As the CO_2 is released form the underground storage and flows towards the methanation process, an expansion turbine utilizes the volumetric work. The CO_2 is preheated by the thermal storage and less heating energy is needed for the methanation. In fact, a deeper storage is beneficial, since the geothermal heat can be utilised and the process efficiency increases. Such combination of geothermal energy production with supercritical CO_2 injections has been investigated elsewhere.[97,98] Nevertheless, the additional equipment cost for compressor, thermal storage and the turbine need to be considered in subsequent studies. Therefore, further studies will investigate the energetic assessment of the storage from a thermo-economical perspective.

Storage of O_2 and H_2. As a by-product of the high temperature electrolyser, O_2 is considered as a vital technical gas and its short-term storage is crucial for the overall process. Pure O_2 will be used in the GtP section during the oxy-combustion step and substantial storage capacities for O_2 have to be held available for the operation of the storage system. Gaseous storage of O_2 requires exceptionally large storage volumes that only could be met by subsurface caverns or aquifers. Very little literature exists regarding the feasibility of O_2 storage in caverns, but this question often arises in other PtG studies.[99] Due to the high reactivity of O_2 and therefore chemical interactions with the surrounding rock and liquids present in a subsurface storage, it is likely that the stored O_2 is consumed and possibly dangerous by-products are formed, leading to concerns with respect to the operating safety of the store and its environmental impact. The use of this kind of large-scale storage for O_2 is deemed unviable.

Technical storage of O_2 is typically carried out using high-pressure cylinders, tube trailers or large spherical tanks for stationary applications, depending on the required frequency and rate of consumption. For larger needs like the ones expected in the discussed PtG–GtP system, cryogenic storage of liquid O_2 is a relevant storage option. Yet still, the scale of the

required cryogenic equipment and number of storage tanks within in one single plant location is expected to far exceed typical O_2 storage sites in operation today. To circumvent the previously laid out problems, the storage volume per site could be limited and the bulk of the required O_2 for the oxy-combustion process could be provided by a separate ASU as shown in Table 2 in Section 3.3.

Hydrogen storage is necessary if the electrolyser and the methanation process cannot be coupled perfectly or if additional H_2 is extracted from the PtG cycle for other applications, such as steel production, chemical industry and mobility. However, as H_2 storage is not a central element of the analysed storage power plant concept and is only needed in smaller quantities, any details on respective storage technologies will be omitted.

4. Forecast study: Germany 2050

4.1 General information

The German action plan to achieve greenhouse gas neutrality by 2050 is based on significantly and permanently reducing energy demand, using renewable energy in all sectors, and efficient use of electricity from renewable energy sources in heat provision, transport, and industry.[100] Over the past years, the production of renewable electricity in Germany has grown substantially. Its share of the annual net total increased from 30.2% to 43.9% between 2015 and 2019.

According to the energy transition plan of the German government, renewable energy sources are expected to cover at least 65% of the electricity production in 2030, and 80% in 2050.[101] These goals require the installation of large amounts of generation capacity, namely as photovoltaic panels and wind turbines. The volatility of these technologies calls in turn for the large-scale implementation of energy storages to maintain a reliable supply of electricity.

One of the main contributing factors influencing the national energy balance in 2050, aside from the installed renewable capacities will be the evolution of the overall electricity demand within the next decades. A wealth of different national studies attributed to the detailed future development of the energy system of Germany can be found elsewhere.[102–105] This forecast employs a reference scenario that assumes a significant increase of the electricity demand in Germany until the year 2050. The overall electricity consumption in Germany (Fig. 5) will increase up to approx. 964 TW h by 2050 according to ref. 106.

Although the base consumption of electricity will remain the same until 2050, the consumption due to sector coupling effects (power to X (PtX), heat and transportation sector) will steadily increase. This reference scenario agrees with other recent national studies.[107] Based on the electricity consumption forecast of the aforementioned reference study, an approximate projection of the German energy balance until 2050 based on electricity generation data of the year 2019 has been assessed.

4.2 Assessed scenarios

Since the proposed PtG–GtP system is based on the utilization of CO_2 in a closed loop, this forecast aims to predict the amount of the required renewable capacities and the corresponding residual load profiles to enable a near-CO_2-neutral system operation. This work assesses two different energy system scenarios for the year 2050 and their schematic representations are depicted in Fig. 6.

In both scenarios (Fig. 6), the production of CO_2 through the combustion process of the SNG-fired power plant is equal to the CO_2 intake of the methanation process. In order to achieve this, while covering electricity demand at all times, sufficient capacities for both electrolysis and renewable electricity production have to be provided. The overall carbon inventory attributed to the plant operation remains constant and no permanent CO_2

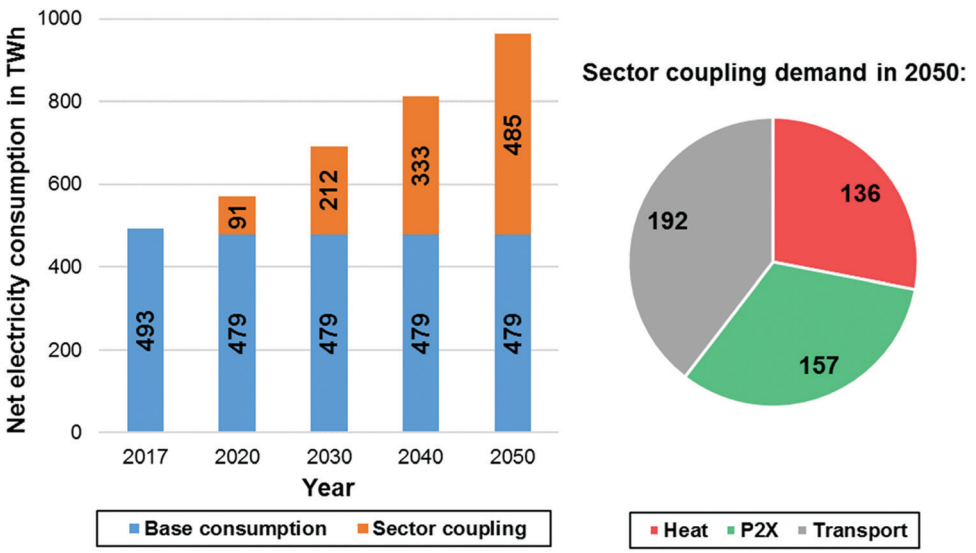

Fig. 5 Net electricity consumption in Germany (left) and sector coupling demands in TW h for 2050 (right) according to ref. 106.

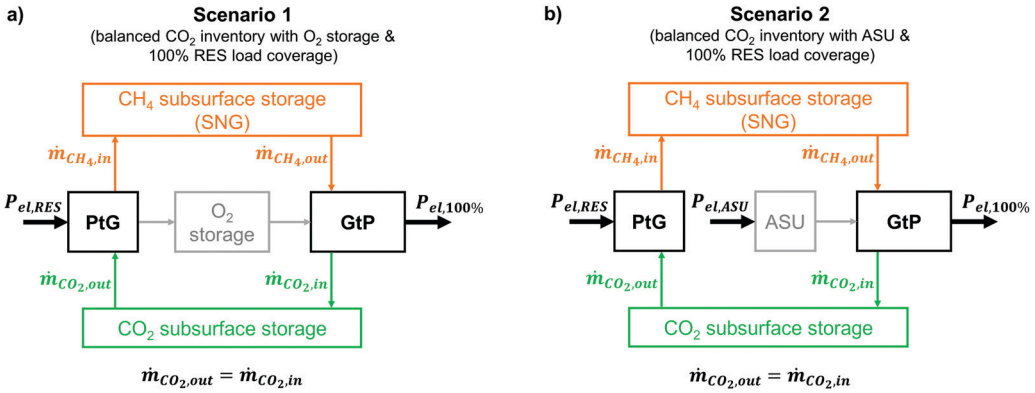

Fig. 6 Assessed energy system scenarios.

storage as well as no additional CH_4 source is needed during system operation. Both scenarios represent a fully renewable energy system (100% renewable energy sources; RES) and the storage system is expected to solely cover the national energy demand at all times and the respective renewable generation capacities in each decade are chosen accordingly.

In the first scenario (Fig. 6a), O_2 produced *via* electrolysis during times of negative residual loads is stored in a dedicated technical storage for later reuse in the GtP reconversion step. In contrast, the second scenario (Fig. 6b) makes use of an ASU for O_2 supply during positive residual loads, requiring additional electrical power for its continuous operation. The excess O_2 from the PtG process is expected to be sold and/or instantly used for other industrial processes. Apart from the different O_2 supply, scenario 1 and 2 share the same boundary conditions.

The forecast is based on data taken from the SMARD platform of the German Bundesnetzagentur (which reflects the same data as the transparency platform ENTSO-E of the European Union).[108] Employed data sets are time series of the net electricity generation, consumption and export/import flux in MWh as well as the installed generation capacities in MW for 2019. The forecast is carried out for the years of 2021 to 2050.

The required power installations for the electrolysis/methanation step as well as for the reconversion step have been determined. All assessed cases require the existence of a non-permanent subsurface CO_2 storage. Moreover, the acquired forecast data is used for the subsequent analyses of the subsurface storage potentials and requirements of CH_4 and CO_2 as well as the technical storage of O_2.

The scenarios presented in this work are intended as a basic orientation and an instrument to verify the plausibility of the combined subsurface gas and energy storage system with respect to the required storage capacities and renewable generation capacity on the national scale of Germany.

4.3 Renewable electricity production and load profiles

To obtain scalable renewable production reference data reflecting basic meteorological patterns and features, the net renewable production time series (E_{RES}) were normalized to the installed capacity of each individual generation type of the respective base year (P_{RES}) according to eqn (5).

$$\hat{E}_{RES}(t) = \frac{E_{RES}(t)}{P_{RES}} \quad (5)$$

Afterwards, the normalized production time series ($\hat{E}_{RES}$) were used to calculate the future renewable power generation time series ($E_{RES,y}$) for any given installed capacity ($P_{RES,y}$) in the forecasted period based on eqn (6).

$$E_{RES,y}(t) = \hat{E}_{RES} \cdot P_{RES,y} \quad (6)$$

According to the German Renewable Energy Federation, the annual growth in renewable capacity until 2030 will be mainly dominated by wind and PV installations, whereas hydroelectric power generation and other forms of renewable generation will only exhibit small growth rates and show signs of saturation.[107] The expected annual capacity extensions shown in Table 4 were used as initial values to determine the actual capacity to reach the goals of each respective scenario.

The installed renewable capacity in the respective year was calculated using eqn (7) cumulating the annual capacity extensions (ΔP_{RES}) until the forecasted year.

$$P_{RES,y} = P_{RES} + \sum \Delta P_{RES} \quad (7)$$

To roughly meet the electricity consumption forecast of the reference study[106] shown in Section 4.1, the actual net consumption time series of the base year (E_{load}) was linearly scaled ($f_{load} = 2$) until 2050 (Table 5) assuming the annual increase in load is evenly distributed across the forecasted 30 year time span. The load time series in 2050 ($E_{load,2050}$) was calculated based on eqn (8) and the cumulative energy demand ($e_{load,2050}$) was calculated according to eqn (9).

$$E_{load,2050}(t) = E_{load}(t) \cdot f_{load} \quad (8)$$

$$e_{load,2050} = \int E_{load,2050}(t)\,dt \quad (9)$$

The aimed consumption of 964 TW h is exceeded in the base year 2019. The scaled load profiles were used for the subsequent calculation of the residual load profiles.

Table 4 Annual renewable installation capacities and total installed capacities of the base year 2019.[107,108] The expected annual growth rates according to ref. 107 are used as initial values for the forecast studies. Calculated renewable capacity extensions that are discussed later may differ from the chosen initial values

	Capacity installed in GW (P_{RES}) in 2019	Expected annual growth in MW (ΔP_{RES})
Biomass	7.75	600
Hydroelectric	5.28	50
Wind (offshore)	6.39	1200
Wind (onshore)	52.79	4700
PV	45.30	10 000
Other	0.49	50

Table 5 Forecast of the cumulative electrical energy demand/consumption for 2030, 2040 and 2050

	Annual demand in TW h ($e_{load,y}$)
Base year	2019
Base year consumption	485
2030	657
2040	813
2050	970

4.4 Residual load profiles and CO_2 load curves

The national residual load profile (R_y) has been defined as the difference between the scaled load time series ($E_{load,y}$) and the scaled net renewable electricity production time series ($E_{RES,y}$).

$$R_y(t) = E_{load,y}(t) - E_{RES,y}(t) \quad (10)$$

To compensate large fluctuations and peaks of the residual load profile, different grid flexibility resources as well as export and import of electrical energy were used to specifically shape the residual load profile.

The transmission capacities of export and import with neighbouring countries will most likely increase in the upcoming decades.[109] Thus, this forecast includes smoothing of the residual load profiles during peak loads *via* import and export. To implement this, time series for imported (E_i) and exported (E_e) amounts of electricity have been included in the model. They are based on the physical net flux of import and export with all neighboring countries of Germany in the respective base year. To reflect the increase in transmission capacities, the import and export time series have been linearly scaled expecting an increase by 50% until the year 2050 ($f_{e,2050}$= 1.5). Furthermore, additional peak load capacities were introduced for both scenarios to account for other forms of grid flexibility resources, which, in fact, will coexist with the proposed PtG–GtP plant. The peak load capacities ($E_{p,max}$ & $E_{p,min}$) will reach a value of 30 GW in 2050, and increase gradually over the course of the forecasted period. Residual load smoothing *via* pumped hydroelectric storage was not considered. All measures with respect to residual load smoothing are reflected in eqn (11).

$$\tilde{R}_y(t) = R_y(t) + (E_i(t) - E_e(t))\cdot f_{e,y} + E_{p,max,y}(t) - E_{p,min,y}(t) \quad (11)$$

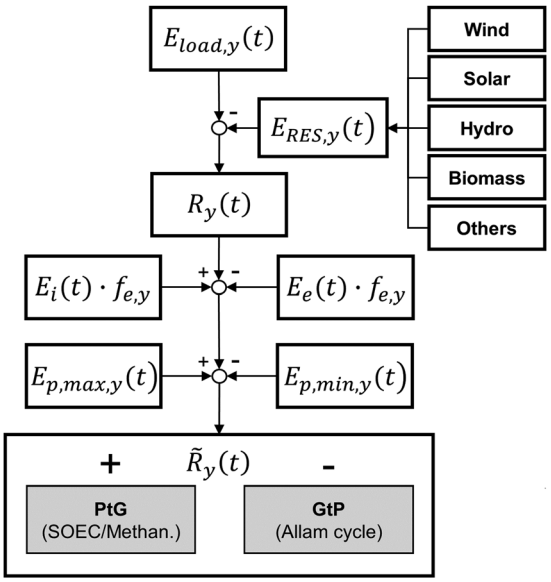

Fig. 7 Applied methodology for the calculation of residual load profiles.

The residual load profile calculation methodology is summarised in Fig. 7.

The resulting residual load profiles are combined with a simple model of the energy plant to specify the demand and the output of CO_2 attributed to processing and subsurface storage. According to Gruber *et al.*, the overall efficiency of a coupled process comprising high temperature electrolysis and a downstream catalytic methanation with close heat integration can reach system efficiencies of up to η_{PtG} = 82%.[59] During times of negative residual loads, the system produces H_2 through the SOEC with an immediate downstream synthesis of CH_4. The SOEC model assumes a constant operation at a cell voltage of φ_{SOEC} = 1.3 V. The required amount of CO_2 retrieved from the subsurface storage ($\dot{m}_{CO_2,out}$) is calculated based on the H_2 output of the SOEC (Faraday's law) and the stoichiometry of the methanation reaction (eqn (2)) according to eqn (12).

$$\dot{m}_{CO_2,out} = \frac{|\tilde{R}_y(t)|\cdot\eta_{PtG}\cdot M_{CO_2}}{\varphi_{SOEC}\cdot z\cdot F\cdot\nu_{H_2}} \quad \text{for } \tilde{R}_y(t) < 0 \quad (12)$$

In case of positive residual loads, the Allam GtP half cycle is operated. The efficiency of the overall GtP reconversion cycle η_{GtP} has been set to 66.1% (scenario 1) and 59.8% (scenario 2) according to the descriptions of the previous sections. The output of CO_2 due to the combustion of CH_4 ($\dot{m}_{CO_2,in}$) was calculated based on the residual power requirements, the LHV (0.802 MJ mol^{-1}) of CH_4 and the stoichiometry of the oxy-combustion reaction (eqn (4)) according to eqn (13)

$$\dot{m}_{CO_2,in} = \frac{\tilde{R}_y(t)\cdot M_{CO_2}}{\eta_{GtP}\cdot LHV_{CH_4}} \quad \text{for } \tilde{R}_y(t) > 0 \quad (13)$$

Thus, the initial residual load profile can be converted into a CO_2 load curve representing the distribution of charge (positive residual loads) and discharge (negative residual loads) quantities of CO_2 from the subsurface storage. The roundtrip

efficiency of the process is expected to be 54.2% (scenario 1) and 49.0% (scenario 2). As previously stated, the annual renewable production capacity extensions are gradually increased starting with the expected values shown in Table 4. For both scenarios, the annual growth rate (assuming constant capacity growth across the forecasted decades) of all renewable generation types was increased until the CO_2 demand of the PtG process met the CO_2 output of the GtP process in the year of 2050 according to the following condition:

$$|\dot{m}_{CO_2,out} - \dot{m}_{CO_2,in}| \leq 0.001 \quad (14)$$

The presented calculation methodology was developed within Matlab 2017b and all simulations have been carried out using this software.

5. Results

5.1 Scenario 1: O_2 storage

To match the CO_2 demand of the PtG process and the CO_2 output of the GtP process in the year of 2050 and thus reaching full circularity, the required annual renewable capacity extensions need to be increased compared to the initially expected annual growth rates according to ref. 107 (Table 6).

To reach a 100% renewable electricity generation in Germany in 2050, 30.1 GW of biomass, 52.2 GW of offshore wind, 227.5 GW of onshore wind and 416.9 GW of PV capacity must be installed and a total annual renewable capacity growth of 20.5 GW has to be maintained beginning in 2021. The total installed renewable generation capacity would have to rise from 118 GW in 2019 to approx. 736 GW in 2050 (Fig. 8).

Due to the forecasted amount of installed renewable capacities in 2050, the residual load profiles are significantly distorted with respect to their power amplitude in comparison to the current state. Fig. 9 shows the residual load profile over the course of the year 2050 for the base year of 2019.

It is evident that the main part of the load can be directly provided by renewable sources, and that renewable electricity production will exceed conventional electricity production by far. However, there are still sustained times during the year characterized by positive residual loads. This means periods of insufficient renewable electricity production and the need for conventional production capacities. Moreover, the residual load profile shows high frequency oscillations, especially during the summer months. This is due to the increased photovoltaic electricity generation caused by the high PV installation

Table 6 Expected and actual capacity extensions to reach a balanced CO_2 inventory

	Expected annual growth in MW[107]	Required annual growth in MW
Biomass	600	741
Hydroelectric	50	62
Wind (offshore)	1200	1482
Wind (onshore)	4700	5804
PV	10 000	12 348
Other	50	62

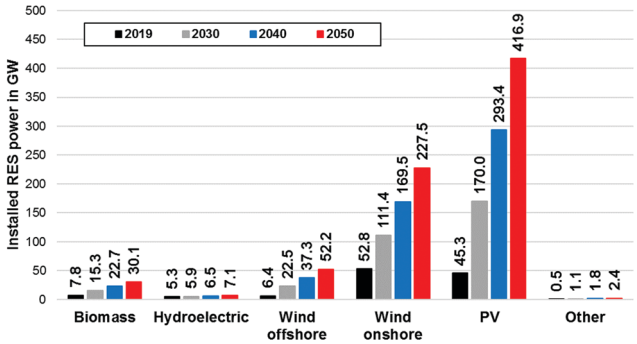

Fig. 8 Simulated renewable installations in 2030, 2040 and 2050 for scenario 1.

capacity and increased sun exposure during daytime. The highest values during positive peak load times appear predominantly during winter. In 2050 the maximum peak load would be 92 GW. On the contrary, the negative peak powers occur during the summer months and a minimum residual load of −264 GW can be observed. Since fixed capacities for peak residual load management were employed, the capacity of the GtP process (positive residual loads) and the total required electrolysis capacity for the PtG process (negative residual loads) can be derived from Fig. 9 on the national scale of Germany. The required electrolysis power installations would have to be as high as 234 GW in 2050 whereas the installed capacity for the power generation cycle would have to be 62 GW. Thus, the required electrolysis capacity exceeds the respective capacity of the GtP step by a factor of approx. 4.

The CO_2 load profile (Fig. 10) clearly reflects the same oscillatory behavior as the residual load profile. The maximum charge and discharge rates of CO_2 range from −18.5 to 30.3 kilotons per hour. To further elaborate the characteristics of the energy production, the annual load duration curves for the years 2019, 2030, 2040 and 2050 are shown in Fig. 11.

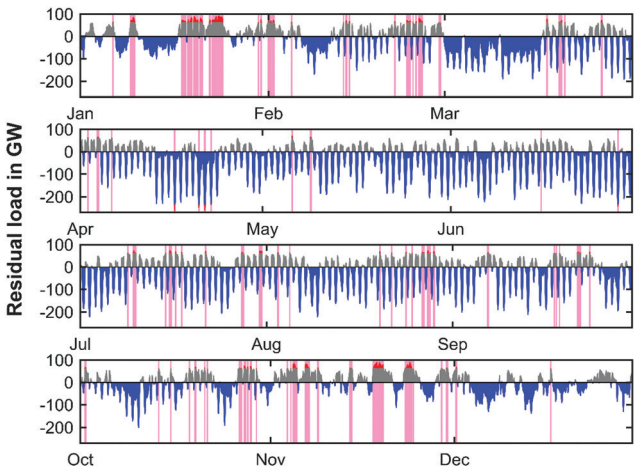

Fig. 9 Simulated residual load profile (2050) with PtG operation (blue; negative residual load), GtP operation (grey; positive residual loads) and peak residual load management (red) for scenario 1. Pink vertical streaks indicate presence of peak residual load management.

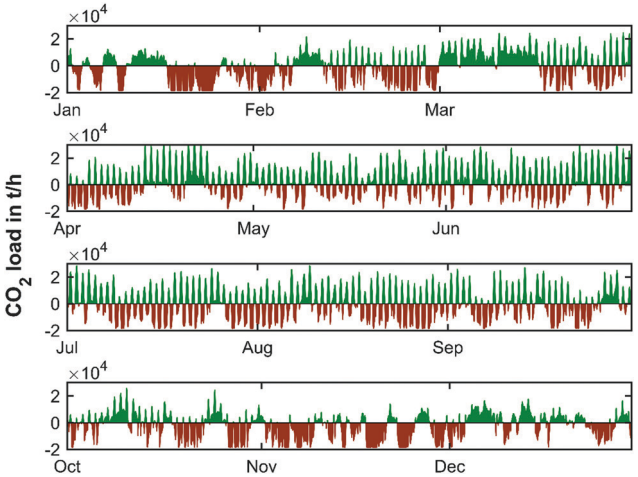

Fig. 10 Simulated CO_2 load profile (2050) for scenario 1.

Because of the steady increase of renewable production capacities, the periods with negative residual loads show a distinct increase over the forecasted time span. As it can be seen in Fig. 11 electrolysis capacities of 66 GW, 150 GW and 234 GW must be installed before the end of 2030, 2040, and 2050 respectively. The required electrolysis power could be reduced through the introduction of additional peak load storage capacities during times of negative residual peak loads. In contrast to this, the required conventional production capacities remain unaffected (62 GW) over the course of the forecast window, provided that sufficient peak load capacities are available each year. A summary of the overall energy balance of the PtG–GtP system for the forecasted year of 2050 based on the reference year 2019 can be found in Table 7.

To allow for a near carbon-neutral system operation under the presented boundary conditions, the installed renewable capacity as well as the amount of electricity produced by renewables must exhibit a substantial increase in the upcoming decades. The total electricity produced by renewable sources in 2050 will be 1200 TW h with installed production capacities of 736 GW. The ratio between the renewable production and load

Table 7 Energy balance of the proposed storage system in the year 2050 under assumption of a carbon-neutral system operation (scenario 1)

Reference year	2019
Renewable capacity (total) in GW	736
Load in TW h	970
Renewable production in TW h	1200
GtP production in TW h	140
PtG demand in TW h	323
Net export in TW h	51
Net peak load cut-off in TW h	4
Renewable production to load ratio (—)	1.22

is found to be 1.22, meaning that in a 100% renewable energy system, renewable production will exceed the respective consumption. It becomes clear that the presented scenario requires entirely different future renewable generation capacities than the current national energy strategy of Germany considers (see Section 4.1). The amount of conventional electricity production will be exclusively provided by SNG-fired Allam cycle power plants and is reduced to approximately 50% compared to the base year production value. The annual electricity demand for the PtG step equals 323 TW h in the year 2050.

The smallest storage volume is found so that the storage site is never over- or under-capacity. This is given by the maximum value at the peak of the CO_2 curve added to the absolute value of the (negative) trough of the cumulative CO_2 curve. Matched here to the cumulative CO_2 curve obtained from the yearly weather pattern of 2019, this represents a characteristic storage quantity of 10 754 kilotons of CO_2. The yearly charging cycle of the temporary storage of CO_2 in this scenario is displayed in Fig. 12 (top).

The concept proposed in the paper applies to a single localised power plant. It can be therefore expected that for a single plant location, the renewable energy availability and corresponding CO_2 load curve is tied to the renewable capacity in the vicinity of the plant. It is assumed that 20 equivalent plants will share the CO_2 load curve equally. For each plant, the corresponding regional CO_2 load curve is then the national load curve divided by a factor of 20. Regional differences in weather

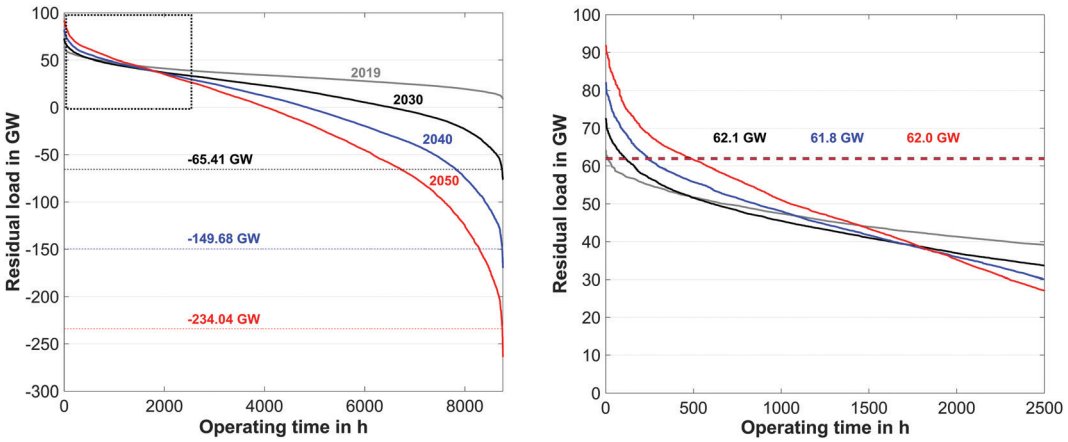

Fig. 11 Annual load duration curve for the years 2019, 2030, 2040 and 2050 based on the reference data of 2019 (left) and detailed view (right).

patterns and renewable energy capacity are also expected to create regional CO_2 load curves that differ. These differences are not considered in the current study.

At typical salt cavern depth of 800 meters, geostatic pressure is approximately 170 bars and temperature is of 34 °C,[110] CO_2 reaches a density of 843.73 kg m^{-3},[111] leading to a characteristic cavern geometrical volume for CO_2 of 637 290 m^3 (271.6 million N m^3). This value, with an added cushion volume of 30%, represents approximately the upper limit of a technically feasible cavern (~1 million m^3). Considering multiple caverns can be created and used in parallel for a single storage location, this value does not appear to be technically prohibitive. While using a large capacity individual cavern or a connected series of smaller caverns at each facility location may be technically feasible for certain regions, given the large salt cavern potential in northern Germany, this seems unfeasible in other German regions (see Section 3.4). Furthermore, high-value salt caverns maybe preferentially used for other types of gas storage rather than CO_2. For this scenario, a porous storage option would be preferred, such as a disused oil and gas field or a porous aquifer, of which Germany has an abundance of potential, in which CO_2 is injected and recovered *via* a geological trap.

Large-scale storage of high-value CH_4 is however expected to be carried out solely *via* salt caverns. The yearly charging cycle for CH_4 is shown in Fig. 12 (bottom). The characteristic maximum storage quantity is determined to be 5211 kilotons with an average CH_4 quantity of 3200 kilotons and a minimum quantity of 1300 kilotons inside the salt cavern, based on the chosen initial storage value of CH_4. Therefore, the required net storage quantity for CH_4 is determined to be 3911 kilotons (equal to 54.5 TW h). Assuming an average cavern storage pressure of 200 bar at a temperature of approximately 30 °C, CH_4 reaches a density of 152 kg m^{-3},[112] the required net underground storage volume for CH_4 is estimated to be approx.

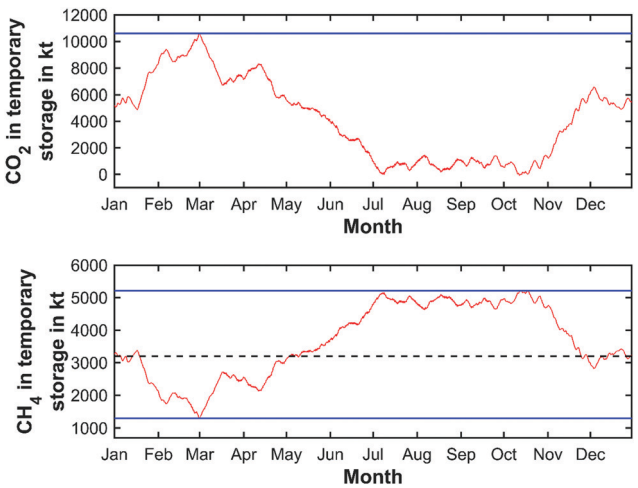

Fig. 12 Cyclical charging and discharging of CO_2 and CH_4 storage on a national scale (the upper blue lines indicate the storage capacities required; the lower blue line indicates the minimum storage quantity of CH_4 and the dashed black line represents the average stored quantity of CH_4 in the subsurface storage based on the chosen initial storage value).

25.8 million m^3 (5.5 billion N m^3) on the national scale. Adding the required cushion gas volume, a total storage volume of 36.9 million m^3 (7.8 billion N m^3) has to be held available nationwide. Considering the total available CH_4 storage available in Germany today (27.4 billion N m^3 [93]), the application of the circular power plant concept appears as a viable option for large-scale electricity storage in the future. Dividing the total storage requirements according to the previously mentioned number of operating sites, 1.9 million m^3 (0.4 billion N m^3) of storage volume have to provided at each site, leading to 2 maximum capacity caverns per plant location.

The storage quantity for O_2 is retrieved in the same manner, leading to a total quantity of approx. 15 650 kilotons to be stored. Since the charging and discharging of the O_2 store exhibits the same temporal fluctuations as seen in Fig. 12, the respective diagram is not shown here. Assuming cryogenic and liquid storage at ambient pressure conditions and a maximum tank size of 1500 m^3, a total storage volume of 13.7 million m^3 or 9140 maximum size tanks (approx. 460 per plant site) has to be provided. A summary of the required storage capacities for all relevant gases/liquids can be found in Table 8.

From a techno-economical and safety standpoint, the application of cryogenic O_2 storage at the determined locational plant scale is not considered as a viable option for a potential and applicable system design.

5.2 Scenario 2: O_2 provision *via* air separation unit

Since the previously presented scenario revealed challenging storage requirements with respect to the cryogenic storage of O_2, the second scenario utilises an ASU instead of stationary O_2 storage. Apart from the adjusted GtP efficiency of the Allam cycle reconversion step to 59.8%, no changes have been made to the forecast calculation. A comparison between the retrieved

Table 8 Total required temporary storage capacities for scenario 1. The total storage volume includes an added cushion gas volume of 30% for CO_2 and CH_4

Gas	Storage quantity in kilotons	Storage volume in m^3	Storage volume in N m^3
CO_2 (gaseous)	10 754	18.2 million	7.8 billion
CH_4 (gaseous)	3911	36.9 million	7.8 billion
O_2 (liquefied)	15 650	13.7 million	—

Table 9 Comparison of the simulated PtG, GtP and renewable capacities in 2050

Scenario	Required PtG installations in GW	Required GtP installations in GW	Required renewable energy sources capacities installation in GW
1	234	62	736
2	243 (increase: 3.85%)	62 (increase: —)	752 (increase: 2.17%)

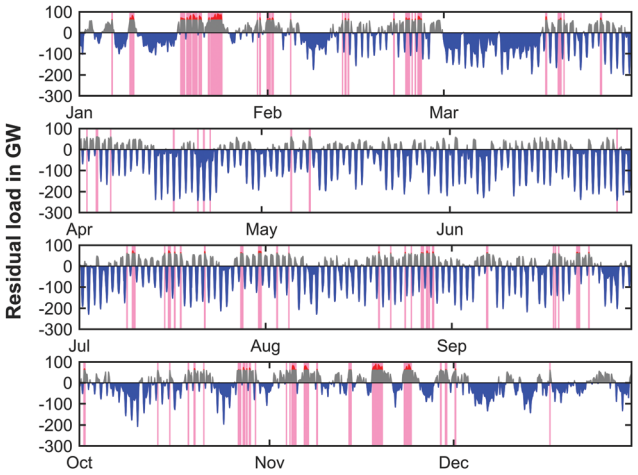

Fig. 13 Simulated residual load profile (2050) with PtG operation (blue; negative residual load), GtP operation (grey; positive residual loads and peak residual load management (red) for scenario 2).

PtG, GtP and renewable capacites for both scenarios is tabulated in Table 9.

Due to the reduction of the efficiency of the reconversion step from 66.1% to 59.8%, the required renewable energy sources installation to meet a balanced CO_2 load curve by 2050 exhibit an increase of 16 GW to 752 GW. To provide sufficient capacities for the production of CH_4, the installed electrolysis capacity will have to be as high as 243 GW, exceeding the previously determined value by 9 GW. The required GtP capacities show no changes and remain at 62 GW. The simulated residual load profiles for the year of 2050 and the balanced scenario based on an ASU is shown in Fig. 13.

The residual load progression across the forecasted year based on the system with an ASU only shows minor deviations when compared to the progression of the system with O_2 storage presented in Fig. 9. It can be noticed that the times where peak load management occurs (pink bands) is slightly reduced and hence the net peak load cut-off is lowered. Since the deviation of the CO_2 load curve only exhibits barely noticeable changes, the respective data is not shown here.

The retrieved values for the required storage quantities of CO_2 and CH_4 are summarised in Table 10. Through the introduction of the ASU to the reconversion system and the lowered roundtrip efficiency, the required storage volumes for CO_2 and CH_4 are increased by 4.24% compared to the balanced scenario with O_2 storage.

The additionally required storage capacities for CO_2 and CH_4 are considered manageable with respect to the available subsurface storage capacities in Germany. Although not covered in the presented scenario, the required additional PtG and renewable capacities (9 GW and 16 GW) could also be covered by import of either electricity or renewable H_2 or CH_4 from neighbouring countries. The respective choice between capacity extensions of PtG and renewable generation within Germany or the extension of transmission capacities for electricity and gas is governed by political and economic aspects, which were not part of this basic study.

Table 10 Total required temporary storage capacities for scenario 2. The total storage volume includes an added cushion gas volume of 30% for CO_2 and CH_4

Gas	Storage quantity in kilotons	Storage volume in m^3	Storage volume in N m^3
CO_2 (gaseous)	11 210 (increase: 4.24%)	19.0 million	8.1 billion
CH_4 (gaseous)	4077 (increase: 4.24%)	38.4 million	8.1 billion

6. Conclusions

In this paper, a large-scale PtG–GtP energy storage concept featuring sCO_2 driven power cycles entangled with subsurface storage facilities for CO_2 and CH_4 has been presented. As negative residual loads occur, electricity is used to generate H_2 by electrolysis from water, which is subsequently used to produce synthetic CH_4 from CO_2 within a Sabatier process. A large subsurface storage supplies CO_2 to the reaction and the produced CH_4 is temporarily stored in underground caverns. As renewable production exceeds demand and positive residual loads occur, CH_4 is withdrawn from the cavern storage and used to drive an Allam power cycle to produce electricity. The CO_2 produced by the power cycle *via* oxy-combustion is fed back to the temporary subsurface storage, thus enabling a circular usage of CO_2 and CH_4.

To achieve an energy storage cycle with confined use of carbon through continuous storage and retrieval of CO_2/CH_4 from the temporary subsurface store, the total installed renewable power must be as high as 736 GW (scenario 1) and 752 GW (scenario 2) in 2050 – far exceeding Germanys installations today. Besides that, both assessed scenarios require large amounts of electrolysis installations to maintain full material circularity until 2050, with required installations being as high as 234 GW and 243 GW. The characteristic CH_4 storage quantity is determined to be 3,911 kilotons (scenario 1) and 4077 kilotons (scenario 2), which corresponds to a storage capacities of 54.5 TW h and 56.7 TW h, respectively. The required CO_2 storage quantities have been determined to be 10 754 kilotons and 11 210 kilotons for scenario 1 and 2, respectively. It was found that the existing and potential storage capacity in Germany today's more than sufficient for the storage of large amounts of CO_2 and CH_4.

The Allam cycle combined with air separation unit was identified as the most viable option for the GtP reconversion process, allowing stand-alone efficiencies of up to 59.8% while the theoretical roundtrip efficiency reaches values of 49.0% (scenario 2).

The combined subsurface storage and circular power plant concept appears as a viable option for large-scale electricity storage in the future. The capacity requirements with respect to the underground gas storages do not exceed the available storage capacity in Germany today. Considering the ongoing expansion of storage infrastructure for CH_4 in Germany in the upcoming decades, the presented storage system architecture becomes a relevant option to cope with the intermittency of

renewable energy sources and the future demand for large-scale energy storage capacities.

Further studies with respect to more detailed system models are planned to reveal the specific operational characteristics of the proposed process scheme as well as their economic implications.

Author contributions

Stefan Fogel: Writing – original draft/investigation/formal analysis/isualization. Christopher Yeates: writing – original draft/investigation/formal analysis/visualization. Sebastian Unger: writing – original draft/investigation/visualization. Gonzalo Rodriguez-Garcia: writing – original draft. Lars Baetcke: writing – original draft. Martin Dornheim: project administration/supervision/writing – review & editing. Cornelia Schmidt-Hattenberger: project administration/supervision/writing – review & editing. David Bruhn: funding acquisition/project administration. Uwe Hampel: funding acquisition/project administration/supervision/writing – review & editing.

Abbreviations

AEL	Alkaline electrolyser
ASU	Air separation unit
BECCS	Bioenergy coupled with carbon capture and storage
CCS	Carbon capture and storage
CCU	Carbon capture and utilisation
CCUS	Carbon capture, utilisation and storage
DAC	Direct air capture
EGR	Enhanced gas recovery
ETS	European trading scheme
RES	Renewable energy sources
GtP	Gas-to-power
LHV	Lower heating value
LNG	Liquefied natural gas
PEM	Proton exchange membrane
PtG	Power-to-gas
PtX/P2X	Power-to-X
sCO_2	Supercritical CO_2
SNG	Synthetic natural gas
SOEC	Solid oxide electrolyser cell
TRL	Technology readiness level
UGS	Underground gas storage

Symbols

e_{load}	Cumulative electricity consumption/load
$e_{load,y}$	Cumulative electricity consumption/load in year y
E_e	Electricity export time series (base year)
E_i	Electricity import time series (base year)
E_{load}	Electricity consumption/load time series (base year)
$E_{load,y}$	Electricity consumption/load time series in year y
$E_{p,max,y}$	Maximum peak load time series in year y
$E_{p,min,y}$	Minimum peak load time series in year y
E_{RES}	Renewable production time series (base year)
$E_{RES,y}$	Renewable production time series in year y
$\hat{E}_{RES}$	Normalised renewable production time series (base year)
$f_{e,y}$	Ex- and import scaling factor in year y
f_{load}	Electric load scaling factor
F	Faraday constant
LHV_{CH_4}	Lower heating value of CH_4
$\dot{m}_{CO_2,in}$	CO_2 mass flow rate sent to subsurface storage
$\dot{m}_{CO_2,out}$	CO_2 mass flow rate retrieved from subsurface storage
M_{CO_2}	Molar mass CO_2
P_{el}	Electric power
P_{RES}	Renewable energy installations (base year)
$P_{RES,y}$	Renewable energy installations in year y
ΔP_{RES}	Annual renewable energy capacity extensions
R_y	Residual load time series in year y
$\tilde{R}_y$	Smoothed residual load time series in year y
t	Time
y	Year
z	Charge number/ion valency
η_{GtP}	Gas to power half cycle efficiency
η_{PtG}	Power to gas half cycle efficiency
ν_{H_2}	Stoichiometric coefficient H_2
φ_{SOEC}	Cell voltage SOEC

Conflicts of interest

There are no conflicts to declare.

Acknowledgements

The Helmholtz Climate Initiative (HI-CAM) is funded by the Helmholtz Association's Initiative and Networking Fund. The authors are responsible for the content of this publication.

References

1 Intergovernmental Panel on Climate Change *et al.* Global warming of 1.5 °C. An IPCC Special Report on the impacts of global warming of 1.5 °C above pre-industrial levels and related global greenhouse gas emission pathways, in the context of strengthening the global response to the threat of climate change, 2018.

2 International Energy Agency, "Global CO_2 emissions in 2019," 2020. [Online]. Available: **https://www.iea.org/articles/global-co2-emissions-in-2019**. [Accessed: 11-Feb-2021].

3 J. F.-D. Tapia, J. Y. Lee, R. E.-H. Ooi, D. C.-Y. Foo and R. R. Tan, A review of optimization and decision-making models for the planning of CO_2 capture, utilization and storage (CCUS) systems, *Sustainable Production Consumption*, 2018, **13**, 1–15, DOI: **10.1016/j.spc.2017.10.001**.

4 J. Baek, Do nuclear and renewable energy improve the environment? Empirical evidence from the United States, *Ecol. Indic.*, 2016, **66**, 352–356, DOI: **10.1016/j.ecolind.2016.01.059**.

5 E. I. Koytsoumpa, C. Bergins and E. Kakaras, The CO_2 economy: review of CO_2 capture and reuse technologies,

J. Supercrit. Fluids, 2018, **132**(6), 3–16, DOI: 10.1016/j.supflu.2017.07.029.

6 H. Zhao, X. Liao, Y. Chen and X. Zhao, Sensitivity analysis of CO_2 sequestration in saline aquifers, *Pet. Sci.*, 2010, **7**(3), 372–378, DOI: 10.1007/s12182-010-0080-2.

7 S. Bachu, Screening and ranking of sedimentary basins for sequestration of CO_2 in geological media in response to climate change, *Environ. Geol.*, 2003, **44**(3), 277–289, DOI: 10.1007/s00254-003-0762-9.

8 P. Markewitz, *et al.*, Worldwide innovations in the development of carbon capture technologies and the utilization of CO_2, *Energy Environ. Sci.*, 2012, **5**(6), 7281–7305, DOI: 10.1039/c2ee03403d.

9 T. Hashimoto, S. Ichi Hiramatsu, T. Yamamoto, H. Takano, M. Mizuno and H. Miida, Evaluation of CO_2 Aquifer storage capacity in the vicinity of a large emission area in Japan: Case history of Osaka Bay, *Energy Proc.*, 2009, **1**(1), 2701–2708, DOI: 10.1016/j.egypro.2009.02.039.

10 Y. Fang, B. Baojun, T. Dazhen, S. Dunn-Norman and D. Wronkiewicz, Characteristics of CO_2 sequestration in saline aquifers, *Pet. Sci.*, 2010, **7**(1), 83–92, DOI: 10.1007/s12182-010-0010-3.

11 A. Maia da Costa, *et al.*, Experimental salt cavern in offshore ultra-deep water and well design evaluation for CO_2 abatement, *Int. J. Min. Sci. Technol.*, 2019, **29**(5), 641–656, DOI: 10.1016/j.ijmst.2019.05.002.

12 M. D. Aminu, S. A. Nabavi, C. A. Rochelle and V. Manovic, A review of developments in carbon dioxide storage, *Appl. Energy*, 2017, **208**, 1389–1419, DOI: 10.1016/j.apenergy.2017.09.015.

13 E. Lindeberg, Escape of CO_2 from aquifers, *Energy Convers. Manage.*, 1997, **38**(SUPPL. 1), 235–240, DOI: 10.1016/s0196-8904(96)00275-0.

14 M. Fasihi, O. Efimova and C. Breyer, Techno-economic assessment of CO_2 direct air capture plants, *J. Clean. Prod.*, 2019, **224**, 957–980, DOI: 10.1016/j.jclepro.2019.03.086.

15 E. S. Sanz-Pérez, C. R. Murdock, S. A. Didas and C. W. Jones, Direct Capture of CO_2 from Ambient Air, *Chem. Rev.*, 2016, **116**(19), 11840–11876, DOI: 10.1021/acs.chemrev.6b00173.

16 A. Kumar, *et al.*, Direct Air Capture of CO_2 by Physisorbent Materials, *Angew. Chem., Int. Ed.*, 2015, **54**(48), 14372–14377, DOI: 10.1002/anie.201506952.

17 S. Choi, J. H. Drese, P. M. Eisenberger and C. W. Jones, Application of amine-tethered solid sorbents for direct CO_2 capture from the ambient air, *Environ. Sci. Technol.*, 2011, **45**(6), 2420–2427, DOI: 10.1021/es102797w.

18 C. Breyer, M. Fasihi and A. Aghahosseini, Carbon dioxide direct air capture for effective climate change mitigation based on renewable electricity: a new type of energy system sector coupling, *Mitig. Adapt. Strateg. Glob. Chang.*, 2020, **25**(1), 43–65, DOI: 10.1007/s11027-019-9847-y.

19 N. Mac Dowell and M. Fajardy, On the potential for BECCS efficiency improvement through heat recovery from both post-combustion and oxy-combustion facilities, *Faraday Discuss.*, 2016, **192**, 241–250, DOI: 10.1039/c6fd00051g.

20 C. Gough and P. Upham, Biomass energy with carbon capture and storage (BECCS or Bio-CCS), *Greenh. Gases Sci. Technol.*, 2011, **1**(4), 324–334, DOI: 10.1002/ghg.34.

21 M. Bui, M. Fajardy and N. Mac Dowell, Bio-energy with carbon capture and storage (BECCS): opportunities for performance improvement, *Fuel*, 2018, **213**, 164–175, DOI: 10.1016/j.fuel.2017.10.100.

22 K. Michael, *et al.*, ''Geological storage of CO_2 in saline aquifers-A review of the experience from existing storage operations, *Int. J. Greenhouse Gas Control*, 2010, **4**(4), 659–667, DOI: 10.1016/j.ijggc.2009.12.011.

23 S. Rönsch, *et al.*, Review on methanation – From fundamentals to current projects, *Fuel*, 2016, **166**, 276–296, DOI: 10.1016/j.fuel.2015.10.111.

24 B. Decourt, Weaknesses and drivers for power-to-X diffusion in Europe. Insights from technological innovation system analysis, *Int. J. Hydrogen Energy*, 2019, **44**(33), 17411–17430, DOI: 10.1016/j.ijhydene.2019.05.149.

25 S. Schiebahn, T. Grube, M. Robinius, V. Tietze, B. Kumar and D. Stolten, Power to gas: Technological overview, systems analysis and economic assessment for a case study in Germany, *Int. J. Hydrogen Energy*, 2015, **40**(12), 4285–4294, DOI: 10.1016/j.ijhydene.2015.01.123.

26 S. Weidner, M. Faltenbacher, I. François, D. Thomas, J. B. Skùlason and C. Maggi, Feasibility study of large scale hydrogen power-to-gas applications and cost of the systems evolving with scaling up in Germany, Belgium and Iceland, *Int. J. Hydrogen Energy*, 2018, **43**(33), 15625–15638, DOI: 10.1016/j.ijhydene.2018.06.167.

27 Audi, ''Audi Technology Portal - Audi e-gas.'' [Online]. Available: https://www.audi-technology-portal.de/de/mobilitaet-der-zukunft/audi-future-lab-mobility/audi-future-energies/audi-e-gas. [Accessed: 15-Apr-2020].

28 J. Guilera, J. Ramon Morante and T. Andreu, Economic viability of SNG production from power and CO_2, *Energy Convers. Manage.*, 2018, **162**(6), 218–224, DOI: 10.1016/j.enconman.2018.02.037.

29 G. Gahleitner, Hydrogen from renewable electricity: an international review of power-to-gas pilot plants for stationary applications, *Int. J. Hydrogen Energy*, 2013, **38**(5), 2039–2061, DOI: 10.1016/j.ijhydene.2012.12.010.

30 M. Kuhn, M. Streibel, N. Nakaten and T. Kempka, Integrated underground gas storage of CO_2 and CH_4 to decarbonisethe 'power-to-gas-to-gas-to-power' technology, *Energy Proc.*, 2014, **59**, 9–15, DOI: 10.1016/j.egypro.2014.10.342.

31 M. Kühn, Q. Li, N. Nakaten and T. Kempka, Integrated subsurface gas storage of CO_2 and CH_4 offers capacity and state-of-the-art technology for energy storage in China, *Energy Proc.*, 2017, **125**, 14–18, DOI: 10.1016/j.egypro.2017.08.039.

32 M. Kühn, N. Nakaten, M. Streibel and T. Kempka, CO_2 Geological Storage and Utilization for a Carbon Neutral 'Power-to-gas-to-power' Cycle to Even Out Fluctuations of Renewable Energy Provision, *Energy Proc.*, 2014, **63**, 8044–8049, DOI: 10.1016/j.egypro.2014.11.841.

33 A. Abdon, X. Zhang, D. Parra, M. K. Patel, C. Bauer and J. Worlitschek, Techno-economic and environmental assessment of stationary electricity storage technologies for different time scales,'', *Energy*, 2017, **139**, 1173–1187, DOI: 10.1016/j.energy.2017.07.097.

34 M. Kühn, N. C. Nakaten and T. Kempka, Geological storage capacity for green excess energy readily available in Germany, *Adv. Geosci.*, 2020, **54**, 173–178, DOI: **10.5194/adgeo-54-173-2020**.

35 M. Streibel, N. Nakaten, T. Kempka and M. Kühn, Analysis of an integrated carbon cycle for storage of renewables, *Energy Proc.*, 2013, **40**, 202–211, DOI: **10.1016/j.egypro.2013.08.024**.

36 C. Yilmaz, R. Güttel and T. Turek, Zero-Emissions Power Plant for Chemical Energy Storage as well as Power and Heat Generation, *Chemie Ing. Technol.*, 2015, **87**(4), 419–425, DOI: **10.1002/cite.201400166**.

37 A. Kacludis, S. Lyons, D. Nadav and E. Zdankiewicz, Waste Heat to Power (WH2P) Applications Using a Supercritical CO_2-Based Power Cycle, *Power-Gen Int.*, 2012, **2**, 1–10.

38 G. Subbaraman, *et al.*, ZEPS TM Plant Model: A High Efficiency Power Cycle with Pressurized Fluidized Bed Combustion Process, *2nd Oxyfuel Combust. Conf.*, 2011, 2–5.

39 M. Jentsch, T. Trost and M. Sterner, Optimal Use of Power-to-Gas Energy Storage Systems in an 85% Renewable Energy Scenario, *Energy Proc.*, 2014, **46**, 254–261, DOI: **10.1016/j.egypro.2014.01.180**.

40 M. Thema, M. Sterner, T. Lenck and P. Götz, Necessity and Impact of Power-to-gas on Energy Transition in Germany, *Energy Proc.*, 2016, **99**, 392–400, DOI: **10.1016/j.egypro.2016.10.129**.

41 F. Petipas, A. Brisse and C. Bouallou, Benefits of external heat sources for high temperature electrolyser systems, *Int. J. Hydrogen Energy*, 2014, **39**(11), 5505–5513, DOI: **10.1016/j.ijhydene.2014.01.179**.

42 M. Götz, *et al.*, Renewable Power-to-Gas: A technological and economic review, *Renew. Energy*, 2016, **85**, 1371–1390, DOI: **10.1016/j.renene.2015.07.066**.

43 J. D. Holladay, J. Hu, D. L. King and Y. Wang, An overview of hydrogen production technologies, *Catal. Today*, 2009, **139**(4), 244–260, DOI: **10.1016/j.cattod.2008.08.039**.

44 K. Zeng and D. Zhang, Recent progress in alkaline water electrolysis for hydrogen production and applications, *Prog. Energy Combust. Sci.*, 2010, **36**(3), 307–326, DOI: **10.1016/j.pecs.2009.11.002**.

45 I. Dincer and C. Acar, Review and evaluation of hydrogen production methods for better sustainability, *Int. J. Hydrogen Energy*, 2014, **40**(34), 11094–11111, DOI: **10.1016/j.ijhydene.2014.12.035**.

46 S. D. Ebbesen, S. H. Jensen, A. Hauch and M. B. Mogensen, High temperature electrolysis in alkaline cells, solid proton conducting cells, and solid oxide cells, *Chem. Rev.*, 2014, **114**(21), 10697–10734, DOI: **10.1021/cr5000865**.

47 Ø. Ulleberg, T. Nakken and A. Eté, The wind/hydrogen demonstration system at Utsira in Norway: Evaluation of system performance using operational data and updated hydrogen energy system modeling tools, *Int. J. Hydrogen Energy*, 2010, **35**(5), 1841–1852, DOI: **10.1016/j.ijhydene.2009.10.077**.

48 A. Ursúa, L. M. Gandía and P. Sanchis, Hydrogen production from water electrolysis: Current status and future trends, *Proc. IEEE*, 2012, **100**(2), 410–426, DOI: **10.1109/JPROC.2011.2156750**.

49 M. Carmo, D. L. Fritz, J. Mergel and D. Stolten, A comprehensive review on PEM water electrolysis, *Int. J. Hydrogen Energy*, 2013, **38**(12), 4901–4934, DOI: **10.1016/j.ijhydene.2013.01.151**.

50 J. I. Levene, M. K. Mann, R. M. Margolis and A. Milbrandt, An analysis of hydrogen production from renewable electricity sources, *Sol. Energy*, 2007, **81**(6), 773–780, DOI: **10.1016/j.solener.2006.10.005**.

51 M. Ni, M. K.-H. Leung and D. Y.-C. Leung, An electrochemical model of a solid oxide steam electrolyzer for hydrogen production, *Chem. Eng. Technol.*, 2006, **29**(5), 636–642, DOI: **10.1002/ceat.200500378**.

52 M. Dumortier, J. Sanchez, M. Keddam and O. Lacroix, Energy transport inside a three-phase electrode and application to a proton-conducting solid oxide electrolysis cell, *Int. J. Hydrogen Energy*, 2013, **38**(6), 2610–2623, DOI: **10.1016/j.ijhydene.2012.12.044**.

53 M. Hering, J. Brouwer and W. Winkler, Dynamic model of a micro-tubular solid oxide fuel cell stack including an integrated cooling system, *J. Power Sources*, 2017, **342**, 504–514, DOI: **10.1016/j.jpowsour.2016.11.070**.

54 M. Ni, M. K.-H. Leung and D. Y.-C. Leung, Parametric study of solid oxide steam electrolyzer for hydrogen production, *Int. J. Hydrogen Energy*, 2007, **32**(13), 2305–2313, DOI: **10.1016/j.ijhydene.2007.03.001**.

55 E. Giglio, *et al.*, Power-to-Gas through High Temperature Electrolysis and Carbon Dioxide Methanation: Reactor Design and Process Modeling, *Ind. Eng. Chem. Res.*, 2018, **57**(11), 4007–4018, DOI: **10.1021/acs.iecr.8b00477**.

56 F. Salomone, E. Giglio, D. Ferrero, M. Santarelli, R. Pirone and S. Bensaid, Techno-economic modelling of a Power-to-Gas system based on SOEC electrolysis and CO_2 methanation in a RES-based electric grid, *Chem. Eng. J.*, 2019, **377**, DOI: **10.1016/j.cej.2018.10.170**.

57 D. Parigi, E. Giglio, A. Soto and M. Santarelli, Power-to-fuels through carbon dioxide Re-Utilization and high-temperature electrolysis: a technical and economical comparison between synthetic methanol and methane, *J. Clean. Prod.*, 2019, **226**(6), 679–691, DOI: **10.1016/j.jclepro.2019.04.087**.

58 L. Wang, M. Pérez-Fortes, H. Madi, S. Diethelm, J. Van herle and F. Maréchal, Optimal design of solid-oxide electrolyzer based power-to-methane systems: a comprehensive comparison between steam electrolysis and co-electrolysis, *Appl. Energy*, 2018, **211**(2017), 1060–1079, DOI: **10.1016/j.apenergy.2017.11.050**.

59 M. Gruber, *et al.*, Power-to-Gas through thermal integration of high-temperature steam electrolysis and carbon dioxide methanation - Experimental results, *Fuel Process. Technol.*, 2018, **181**, 61–74, DOI: **10.1016/j.fuproc.2018.09.003**.

60 M. A. Ancona, *et al.*, Thermal integration of a high-temperature co-electrolyzer and experimental methanator for Power-to-Gas energy storage system, *Energy Convers. Manage.*, 2019, **186**, 140–155, DOI: **10.1016/j.enconman.2019.02.057**.

61 M. Bailera, P. Lisbona, L. M. Romeo and S. Espatolero, Power to Gas projects review: Lab, pilot and demo plants

for storing renewable energy and CO_2, *Renewable Sustainable Energy Rev.*, 2017, **69**(2016), 292–312, DOI: 10.1016/j.rser.2016.11.130.

62 B. Miao and S. H. Chan, The economic feasibility study of a 100-MW Power-to-Gas plant, *Int. J. Hydrogen Energy*, 2019, **44**(38), 20978–20986, DOI: 10.1016/j.ijhydene.2019.02.044.

63 International Energy Agency, ''Natural Gas-Fired Power – Analysis,'' 2020. [Online]. Available: https://www.iea.org/reports/natural-gas-fired-power. [Accessed: 24-Sep-2020].

64 H. Termuehlen, *100 Years of Power Plant Development: Focus on Steam and Gas Turbines as Prime Movers*. New York: ASME Press, 2001.

65 R. K. Bhargava, M. Bianchi, A. De Pascale, G. Negri Di Montenegro and A. Peretto, Gas turbine based power cycles - A state-of-the-art review, *Challenges Power Eng. Environ. - Proc. Int. Conf. Power Eng. 2007, ICOPE 2007*, 2007, 309–310, DOI: 10.1007/978-3-540-76694-0_56.

66 Z. Amrollahi, P. A.-M. Ystad, I. S. Ertesvåg and O. Bolland, Optimized process configurations of post-combustion CO_2 capture for natural-gas-fired power plant - Power plant efficiency analysis, *Int. J. Greenhouse Gas Control*, 2012, **8**, 1–11, DOI: 10.1016/j.ijggc.2012.01.005.

67 C. Biliyok and H. Yeung, Evaluation of natural gas combined cycle power plant for post-combustion CO_2 capture integration, *Int. J. Greenhouse Gas Control*, 2013, **19**, 396–405, DOI: 10.1016/j.ijggc.2013.10.003.

68 M. Kanniche, R. Gros-Bonnivard, P. Jaud, J. Valle-Marcos, J.-M. Amann and C. Bouallou, Pre-combustion, post-combustion and oxy-combustion in thermal power plant for CO_2 capture, *Appl. Therm. Eng.*, 2010, **30**(1), 53–62, DOI: 10.1016/j.applthermaleng.2009.05.005.

69 O. Olumayegun, M. Wang and G. Kelsall, Closed-cycle gas turbine for power generation: a state-of-the-art review, *Fuel*, 2016, **180**, 694–717, DOI: 10.1016/j.fuel.2016.04.074.

70 Y. Liu, Y. Wang and D. Huang, Supercritical CO_2 Brayton cycle: a state-of-the-art review, *Energy*, 2019, **189**(6), 115900, DOI: 10.1016/j.energy.2019.115900.

71 P. Wu, *et al.*, A review of research and development of supercritical carbon dioxide Brayton cycle technology in nuclear engineering applications, *Nucl. Eng. Des.*, 2020, **368**(July), 110767, DOI: 10.1016/j.nucengdes.2020.110767.

72 C. White, *Analysis of Brayton Cycles Utilizing Supercritical Carbon Dioxide*, Pittsburgh, PA, and Morgantown, WV (United States), 2014.

73 E. Sun, H. Hu, H. Li, J. Xu and G. Liu, Concept design of supercritical CO_2 cycle driven by pressurized fluidized bed combustion (PFBC) boiler, *Appl. Therm. Eng.*, 2020, **166**, 114756, DOI: 10.1016/j.applthermaleng.2019.114756.

74 Intergovernmental Panel on Climate Change, ''Carbon Dioxide Capture and Storage,'' Cambridge, 2005.

75 U.S. Department of Energy, Supercritical Carbon Dioxide Brayton Cycle, *Quadrenn. Technol. Rev.*, 2015, 1–28.

76 N. Ferrari, L. Mancuso, J. Davison, P. Chiesa, E. Martelli and M. C. Romano, Oxy-turbine for Power Plant with CO_2 Capture, *Energy Proc.*, 2017, **114**(2016), 471–480, DOI: 10.1016/j.egypro.2017.03.1189.

77 L. Mancuso, N. Ferrari, C. Paolo, E. Martelli and M. Romano, *Oxy-combustion turbine power plants*, 2015.

78 R. Allam, *et al.*, Demonstration of the Allam Cycle: An Update on the Development Status of a High Efficiency Supercritical Carbon Dioxide Power Process Employing Full Carbon Capture, *Energy Proc.*, 2017, **114**(2018), 5948–5966, DOI: 10.1016/j.egypro.2017.03.1731.

79 D. Fernandes, S. Wang, Q. Xu, R. Buss and D. Chen, ''Process and Carbon Footprint Analyses of the Allam Cycle Power Plant Integrated with an Air Separation Unit, *Clean Technol.*, 2019, **1**(1), 325–340, DOI: 10.3390/cleantechnol1010022.

80 C. Mitchell, V. Avagyan, H. Chalmers and M. Lucquiaud, An initial assessment of the value of Allam Cycle power plants with liquid oxygen storage in future GB electricity system, *Int. J. Greenhouse Gas Control*, 2019, **87**(6), 1–18, DOI: 10.1016/j.ijggc.2019.04.020.

81 V. Jülch, Comparison of electricity storage options using levelized cost of storage (LCOS) method, *Appl. Energy*, 2016, **183**, 1594–1606, DOI: 10.1016/j.apenergy.2016.08.165.

82 D. Vikara *et al.*, *Underground Natural Gas Storage – Analog Studies to Geologic Storage of CO_2, 2019.*

83 DVV Media Group GmbH, Underground Gas Storage in Germany, *Erdöl Erdgas Kohle*, 2020, **136**(11), 20–25, DOI: 10.19225/201101.

84 H. Plaat, Underground gas storage: Why and how, *Geol. Soc. Spec. Publ.*, 2009, **313**(1), 25–37, DOI: 10.1144/SP313.4.

85 N. Mac Dowell, P. S. Fennell, N. Shah and G. C. Maitland, The role of CO_2 capture and utilization in mitigating climate change, *Nat. Clim. Change*, 2017, **7**(4), 243–249, DOI: 10.1038/nclimate3231.

86 T. Radoslaw, U. M. Barbara and W. Adam, CO_2 storage capacity of deep aquifers and hydrocarbon fields in Poland-EU GeoCapacity Project results, *Energy Proc.*, 2009, **1**(1), 2671–2677, DOI: 10.1016/j.egypro.2009.02.035.

87 T. Takahashi, T. Ohsumi, K. Nakayama, K. Koide and H. Miida, Estimation of CO_2 Aquifer Storage Potential in Japan, *Energy Proc.*, 2009, **1**(1), 2631–2638, DOI: 10.1016/j.egypro.2009.02.030.

88 B. Page, G. Turan and A. Zapantis, *Global Status of CCS 2019 - Targeting Climate Change*, 2019.

89 M. Kühn, A. Liebscher, S. Martens, F. Möller, T. Kempka and M. Streibel, Safe operation of geological CO_2 storage using the example of the pilot site in ketzin, in *Carbon Capture, Storage and Use: Technical, Economic, Environmental and Societal Perspectives*, 60, 6, Cham: Springer International Publishing, 2015, pp. 127–143.

90 K. Müller and C. Reinhold, *Geologische Charakterisierung tiefliegender Speicher- und Barrierehorizonte in Deutschland - Speicher-Kataster Deutschland*. Hannover: Schweizerbart, 2011.

91 S. Knopf and F. May, Comparing Methods for the Estimation of CO2 Storage Capacity in Saline Aquifers in Germany: Regional Aquifer Based vs. Structural Trap Based Assessments, *Energy Proc.*, 2017, **114**, 4710–4721, DOI: 10.1016/j.egypro.2017.03.1605.

92 S. Donadei, *et al.*, Project InSpEE - Rock Mechanical Design for CAES and H_2 Storage Caverns & Evaluation of Storage Capacity in NW-Germany, 2015, 1–5, DOI: 10.3997/2214-4609.201414255.
93 D. G. Caglayan, *et al.*, Technical potential of salt caverns for hydrogen storage in Europe, *Int. J. Hydrogen Energy*, 2020, **45**(11), 6793–6805, DOI: 10.1016/j.ijhydene.2019.12.161.
94 J. Weibezahn, R. Weinhold, C. Gerbaulet and F. Kunz, ''List of conventional power plants in Germany and European countries,'' 2020. [Online]. Available: https://data.open-power-system-data.org/conventional_power_plants/2020-10-01.
95 German Emissions Trading Authority, ''Installations covered by ETS Germany in 2018,'' 2019. [Online]. Available: https://www.dehst.de/SharedDocs/downloads/EN/installation_lists/2018.pdf. [Accessed: 02-Sep-2020].
96 F. Kunz *et al.*, *Electricity, Heat, and Gas Sector Data for Modeling the German System*, 2017.
97 J. B. Randolph and M. O. Saar, Coupling carbon dioxide sequestration with geothermal energy capture in naturally permeable, porous geologic formations: Implications for CO_2 sequestration, *Energy Proc.*, 2011, **4**, 2206–2213, DOI: 10.1016/j.egypro.2011.02.108.
98 N. Garapati, J. B. Randolph, J. L. Valencia and M. O. Saar, CO_2-Plume Geothermal (CPG) Heat Extraction in Multi-layered Geologic Reservoirs, *Energy Proc.*, 2014, **63**, 7631–7643, DOI: 10.1016/j.egypro.2014.11.797.
99 A. Burnol, I. Gravaud, M. Faure and B. Bazargan-Sabet, ''Energy Recovery Through Massive and Reversible Underground Storage (O_2, CO_2, CH_4), in *Electrify Europe Conference*, 2018.
100 Federal Ministry for the Environment, ''Climate Action Plan 2050. Principles and goals of the German government's climate policy,'' 2016.
101 Federal Ministry for Economic Affairs and Energy, ''Sixth 'Energy Transition' Monitoring Report - The Energy of the Future,'' Berlin, 2018.
102 German Environment Agency, ''Germany in 2050 - a greenhouse gas-neutral country,'' Dessau-Roßlau, 2014.
103 T. Smolinka, M. Günther and J. Garche, ''NOW-Studie: Stand und Entwicklungspotenzial der Wasserelektrolyse zur Herstellung von Wasserstoff aus regenerativen Energien,'' 2010.
104 German Environment Agency, ''Energieziel 2050: 100% Strom aus erneuerbaren Quellen,'' Dessau-Roßlau, 2010.
105 J. Ecke, S. Klein, S. W. Klein and T. Steinert, ''Klimaschutz durch Sektorenkopplung: Optionen, Szenarien, Kosten,'' 2017.
106 Leopoldina Nationale Akademie der Wissenschaften, acatech – Deutsche Akademie der Technikwissenschaften, and Union der deutschen Akademien der Wissenschaften, ''Sektorenkopplung - Optionen für die nächste Phase der Energiewende,'' 2017.
107 German Renewable Energy Federation, ''Das BEE-Szenario 2030,'' 2019.
108 Bundesnetzagentur, ''SMARD Electricity Market Data,'' 2020. [Online]. Available: https://www.smard.de/en/downloadcenter/download-market-data. [Accessed: 15-Apr-2020].
109 Fraunhofer Institute for Wind Energy Systems, ''Dynamische Simulation der Stromversorgung in Deutschland nach dem Ausbauszenarion der Erneuerbaren-Energien-Branche,'' 2009.
110 P. Bérest and B. Brouard, Safety of Salt Caverns Used for Underground Storage Blow Out; Mechanical Instability; Seepage; Cavern Abandonment, *Oil Gas Sci. Technol.*, 2003, **58**(3), 361–384, DOI: 10.2516/ogst:2003023.
111 MegaWatSoft Inc, ''CO_2 Tables Calculator.'' [Online]. Available: https://www.carbon-dioxide-properties.com/co2tablesweb.aspx. [Accessed: 27-Jul-2020].
112 National Institute of Standards and Technology, ''Thermophysical Properties of Fluid Systems,'' 2021. [Online]. Available: https://webbook.nist.gov/chemistry/fluid/. [Accessed: 17-Feb-2021].